Pharmacological Research on Therapeutic Agents for Nonalcoholic Steatohepatitis Using a Newly Established Mouse Model

2018

土屋　俊太郎

Table of contents

Chapter 1

Introduction

1.1 Definition and classification of NAFLD/NASH

Nonalcoholic fatty liver disease (NAFLD), one of the most common causes of chronic liver disease worldwide, is characterized by excessive fat accumulation in the liver, referred to as steatosis, in patients without a history of alcohol abuse and infection by hepatitis B virus (HBV) or hepatitis C virus (HCV) [1]. The disease is asymptomatic and usually diagnosed in patients who have received a medical examination based on the elevation of liver aminotransferases or steatosis identified by abdominal ultrasound examination [1,2]. The disease covers a wide spectrum of liver disorders, from simple steatosis to nonalcoholic steatohepatitis (NASH). Simple steatosis, a benign type, has only the histological findings of steatosis, whereas NASH is a more severe and progressive type. In patients with NASH, the disease can progress to cirrhosis, which results in liver failure, portal hypertension, and hepatocellular carcinoma (HCC).

The only method to obtain a definitive diagnosis between steatosis and NASH is a liver biopsy followed by histopathological analysis [3]. Typical histological features of NASH are steatosis, lobular inflammation, hepatocellular ballooning, and fibrosis [4]. Matteoni et al. reported the long-term outcomes of patients with NAFLD classified into four subgroups, based on their hepatic histopathological findings: type 1, fatty liver alone; type 2, fat accumulation and lobular inflammation; type 3, fat accumulation and hepatocellular ballooning degeneration; and type 4, fat accumulation, hepatocellular ballooning degeneration, and either Mallory's hyaline or fibrosis [5]. In their study, the progression to cirrhosis and liver-related deaths was observed almost exclusively in patients diagnosed with types 3 or 4 [5]. Based on the evidence, they proposed the presence of ballooning degeneration, accompanied by fat accumulation and lobular

inflammation, as a definition of NASH. Therefore, ballooning degeneration is currently regarded as a hallmark of NASH.

However, the dichotomous assessment of either having NASH or not, by Matteoni's classification is less helpful for the evaluation of therapeutic agents that may ameliorate NASH in clinical trials. Therefore, a scoring system is required that covers the full spectrum of NAFLD and to quantify histological changes with greater accuracy. To meet this demand, a semiquantitative scoring system of NAFLD activity score (NAS) and fibrosis staging was developed by the NASH Clinical Research Network [6]. NAS is defined as the sum of the scores for steatosis (0–3), lobular inflammation (0–3), and ballooning (0–2); patients with NAS $\geq$ 5 are diagnosed as having NASH. Currently, the scoring system is widely utilized in NAFLD-related clinical trials.

1.2 Clinical importance of NAFLD/NASH

Recent studies have indicated that the prevalence of NAFLD in adults in Western countries was estimated to be between 20% and 40% [1,7–9], which was higher than those in Asian countries [1,7,10–13]. A large, Japanese, multicenter, retrospective study demonstrated that approximately 30% of subjects who received health checkups in Japan were affected by NAFLD [14]. The prevalence of NAFLD varies with age and gender; in general, the prevalence increases with age and is especially higher in men between 40–65 years of age [15]. Recent studies have shown that the prevalence of NAFLD was higher in men than in women [1,14], which contrasted with publication before 1990 reporting that NAFLD was more common among middle-aged women [16–18].

As liver biopsy is limited by the invasiveness and the subsequent histological analysis includes referral bias, it is difficult to determine the true prevalence of NASH. From the limited evidence, which may be subjected to bias, NASH was diagnosed by biopsy in approximately 30% of patients with NAFLD in the U.S.; subsequently, NASH prevalence in adults was estimated to range from 3% to 5% [1,8]. The progression to NASH can increase the risk of cirrhosis, liver failure, and HCC, whereas simple steatosis does not appear to be associated with short-term morbidity or mortality. In particular, approximately 9% to 20% of patients with NASH will subsequently develop liver cirrhosis; 10% of patients with cirrhosis can develop HCC, and 22% to 33% of these patients die of complications of liver failure or require a liver transplant within 5 to 7 years [19].

HCC is the sixth leading cause of cancer and the second leading cause of cancer-related deaths worldwide [20]. Although HCV infection is the leading cause of HCC, some reports have suggested that NASH is the cause of its rapid growth. A retrospective cohort study demonstrated that the proportion of patients undergoing liver transplantation for HCC, secondary to NASH, increased rapidly from 8.3% to 13.5% between 2002 and 2012, whereas that of HCV increased steadily from 43.4% to 49.9% in the U.S. [21]. In 2012, NASH was the second leading cause of HCC leading to liver transplant [21]. Furthermore, novel direct-acting antiviral agents for HCV have recently emerged and showed robust efficacy for sustained virologic response [22]. Given the robust efficacy, the etiology of HCC caused by HCV may decrease over time, whereas that of NASH may increase. Owing to the increased prevalence, NAFLD/NASH should be considered as the next main etiology of cirrhosis and HCC in the near future.

Metabolic syndrome (MS) is a cluster of medical conditions, including obesity,

type 2 diabetes, hypertension, and dyslipidemia. The presence of MS and its individual components is associated with an increased risk of cardiovascular disease (CVD) [23]. Given the spread of Western lifestyle with excessive food intake, especially of junk food, and sedentary habits, particularly in developed countries, the occurrence of MS has increased, and it is estimated that approximately one quarter of the adult population worldwide currently have MS [24].

The comorbidity of NAFLD in patients with MS is high: the prevalence of NAFLD was 80%–90% in obese adults, 30%–50% in patients with type 2 diabetes, and up to 90% in those with hyperlipidemia [25]. Furthermore, the prevalence of NAFLD prevalence is closely related to fasting plasma glucose levels [26]. Accompanied by the above-mentioned increase in the population of individuals with MS, the number of patients with NAFLD has increased. A Japanese cohort study showed that the prevalence of NAFLD identified by using ultrasound increased 2.7-fold between 1994 and 2004 [27]. Owing to the close link with MS and the increasing prevalence, NAFLD has received increasing attention as a hepatic component of MS [28].

The available evidence to indicate the prognosis of NAFLD/NASH is accumulating. A population-based cohort study showed that overall mortality among patients with NAFLD was significantly higher than that in a matched control population [29]. The most common cause of death in patients with NAFLD is CVD [5,29], which may be caused by the high comorbidity of MS and NAFLD given the close link between MS and increased CVD risk. Liver-related diseases have also been studied as the second or third most common cause of death [5,29]. Furthermore, clinical evidence has suggested that the presence of NASH among patients with NAFLD may be a function of their liver-related and overall mortality. In a recent meta-analysis, liver-specific and overall

mortality rates among patients with NAFLD were determined to be 0.77 per 1,000 and 15.44 per 1,000, respectively, whereas those among patients with NASH were 11.77 per 1,000 and 25.56 per 1,000, respectively [30]. A similar relationship between NASH and mortality was also reported by Matteoni et al. [5]. In addition to the presence of NASH, the stage of fibrosis in patients with NAFLD was also significantly associated with death or liver transplantation [31]. These results were suggestive of the close relationship of NAFLD and its histological severity with mortality.

1.3 Pathophysiology of NASH

As mentioned above, some patients with steatosis can progress to NASH, which has the features of inflammation and fibrosis, whereas the majority of patients remain free of inflammation or fibrosis. The natural progression of NAFLD/NASH has not completely been elucidated; in particular, the factors that determine whether a patient will progress to NASH or not are uncertain. To explain the pathophysiology of NASH, Day and James put forward the “two-hit theory” in 1998 [32]. In this theory, the accumulation of fat and fatty acids in the hepatocyte acts as the “first hit” and the sensitization of the liver to further insults acts as the “second hit”. The second hit activates the inflammatory cascade, fibrogenesis, and cell death.

Steatosis, the first hit, may be caused by four main mechanisms: (1) increased supply of free fatty acids (FFAs) from circulation; (2) increased *de novo* lipogenesis; (3) insufficient fatty acid oxidation; and (4) insufficient triglyceride secretion [33,34]. Clinical trials have demonstrated that insulin resistance, defined as a reduced cellular response to insulin, was closely linked to NAFLD [35–37]. First, the increase in lipolysis from adipose tissue owing to insulin resistance and/or increased intake of

dietary fat causes an increase in FFAs in the plasma. The increase in circulating FFAs produced from peripheral lipolysis represents the main source of accumulated triglycerides in the liver [38]. Second, in addition to the increased uptake of FFAs, the transcription of fatty acid synthase in the liver is upregulated owing to insulin resistance in patients with NAFLD, which causes an increase of *de novo* lipogenesis [39]. Third, free fatty acids are metabolized through β-oxidation in the mitochondria of hepatocytes and ω-oxidation in the endoplasmic reticulum. Although metabolism is highly activated in patients with NAFLD, the degradation is insufficient and accumulation of triglycerides occurs [40]. Finally, although hepatic triglyceride accumulation and insulin resistance increase the excretion of fat as very-low-density lipoprotein (VLDL) cholesterol, the excretion of fat is insufficient to normalize hepatic triglyceride content in NAFLD [33,41].

Free radical generation in hepatocytes, the second hit, is caused by insulin resistance and increased FFAs in the liver through the mitochondrial oxidation of fatty acids [42]. The attack of hepatocytes by free radicals releases apoptotic bodies and modified lipoproteins, such as oxLDL, which activate Kupffer cells, a hepatic macrophage [43–45]. Activated Kupffer cells produce cytokines and chemokines, such as tumor necrosis factor-α (TNF-α), interleukin-1β (IL-1β), and monocyte chemoattractant protein-1 (MCP-1), which lead to the recruitment and activation of inflammatory cells such as monocytes and natural killer T cells [46]. Activated Kupffer cells can also accelerate fat accumulation in hepatocytes in a TNF-α- and IL-1β-dependent manner [47,48]. Neutrophils also infiltrate the steatotic liver and are associated with the progression of NASH [49]. A number of clinical and preclinical studies demonstrated that myeloperoxidase (MPO), a lysosomal enzyme produced by

neutrophils, is a key factor of the progression of disease such as hepatocyte injury, inflammation, oxidative stress, and fibrogenesis [50–52].

In addition to its role as the source of FFAs, adipose tissue may also contribute to the development of inflammation and insulin resistance in NASH. In adipose tissues of obese patients, macrophages and lymphocytes are accumulated and secrete cytokines such as TNF-α and IL-6 [53]. Furthermore, the secretion of adiponectin from adipocytes, which regulates insulin sensitivity in the liver and muscle, is decreased in obese patients, and this decrease may accelerate insulin resistance [54].

Hepatocellular injury and inflammation can also trigger the differentiation of hepatic stellate cells into proliferative, migratory, and contractile myofibroblasts, which is known as activation [55]. Transforming growth factor-β (TGF-β) is one of key regulatory factors of hepatic stellate cell activation [56]. Activated hepatic stellate cells have pro-fibrogenic transcriptional and secretory profiles and secrete extracellular matrix (ECM) materials, such as collagen, which accumulate and form scars in the liver [55].

Although the two-hit theory is generally considered a simplified theory to explain NASH pathogenesis, Buzzetti et al. modified this theory into “multiple-hit theory” [57]. The multiple-hit theory is based on two pieces of emerging evidence: that the accumulation of triglycerides in hepatocytes may be a protective mechanism from liver damage and that hepatic inflammation can both precede simple steatosis and be a cause of steatosis. In the theory, the aforementioned multiple factors act in parallel and are synergistically implicated in the pathogenesis and progression of NASH.

1.4 Current status of therapeutic options for NASH

There are currently no approved drugs for the treatment of NASH. According to the practice guidelines of the American Association for the Study of Liver Diseases (AASLD), weight management by lifestyle intervention, including caloric restriction and physical exercise, is the only standard care for NASH [3], and was shown to improve hepatic steatosis, lobular inflammation, ballooning, and NAS of obese patients with NASH in a randomized controlled trial [58]. The goal of body weight loss in the guidelines is a loss of more than 7% of body weight to improve the histological features of NASH, including fibrosis [3]. However, there remains a problem of low compliance with treatment, as only approximately 40% of patients who received this intervention were able to achieve the necessary weight loss goal, despite aggressive dietary counseling and exercise recommendations [59]. Therefore, pharmacological therapies are urgently needed.

In the guidelines of AASLD, vitamin E and pioglitazone are now recommended for the treatment of NASH, although they are not yet approved [3]. Vitamin E is a well-known inhibitor of oxidative stress, a key mechanism of hepatocellular injury and disease progression in patients with NASH. In the trial of pioglitazone versus vitamin E versus Placebo for the Treatment of Nondiabetic Patients with Nonalcoholic Steatohepatitis (PIVENS), vitamin E improved the hepatic features of NASH, such as steatosis, lobular inflammation, hepatocellular ballooning, and NAS in patients with NASH but without diabetes [60]. However, there are also concerns about the long-term safety of vitamin E, as it has been reported to be associated with increased mortality and a modest increase in the risk of prostate cancer [61,62]. In contrast, pioglitazone is a peroxisome proliferator-activated receptor γ (PPARγ) agonist commonly prescribed for

type 2 diabetes. A meta-analysis indicated that pioglitazone was efficacious for the improvement of hepatic histological findings, such as ballooning, fibrosis, lobular inflammation, and steatosis in addition to reducing aminotransferase levels in patients with NASH in multiple randomized, placebo-controlled clinical trials [63]. However, pioglitazone has a side effect of weight gain and presents the risk of bone loss [60,64]. Thus, although there is evidence to support the positive efficacy of both vitamin E and pioglitazone, they also have safety issues. Therefore, their risks and benefits should be considered before starting treatment.

In addition to these two promising drugs, other pharmacological agents have also been tested in clinic, such as metformin, ursodeoxycholic acid, omega-3 fatty acids, and statins. As these agents mainly target the medical features of MS, their repositioning to NASH is theoretically reasonable. However, clinical trials and meta-analyses of these concluded that no trials recorded an improvement of liver histology in patients with NASH in clinical trials, although decreases in serum aminotransferases were found in some trials [65]. Therefore, the AASLD guidelines do not recommend these agents for the treatment of NASH [3].

To address the unmet medical needs for the treatment of NASH, many pharmacological candidates with various mechanisms of action are currently in clinical trials [66]. Obeticholic acid (OCA) and elafibranor are promising agents for NASH therapy that have entered phase III trials. OCA, a farnesoid X receptor (FXR) agonist, is a synthetic variant of a natural bile acid, chenodeoxycholic acid, and has already been approved for primary biliary cholangitis. OCA improved hepatic steatosis, lobular inflammation, hepatocellular ballooning, NAS, and fibrosis in patients with NASH in a multicenter, randomized, placebo-controlled trial (FLINT study) [67]. However, several

safety issues associated with OCA were observed, such as elevated LDL cholesterol and pruritus [67]. Elafibranor is a dual agonist of PPARα and δ, which has exhibited efficacy in animal models of NAFLD [68]. Although elafibranor failed to meet its primary endpoint of a certain percentage disappearance of steatohepatitis without worsening of fibrosis in a randomized, double-blind placebo-controlled trial of patients with NASH (GOLDEN-505 trial), a post-hoc analysis showed that elafibranor met the primary endpoint in subjects with moderate-to-severe NASH with NAS ≥ 4 [69].

1.5 Animal models of NASH

As NAFLD/NASH is a disease in which a variety of cells and soluble factors can be intricately interrelated, as described above, the development of animal models of the disease is critical for a better understanding of the pathophysiology and to validate novel agents for the disease. An ideal animal model of NASH should reflect the features of human NASH, including hepatic histopathology and pathophysiology, as well as the pathogenetic background of human disease. Many rodent models have been established as an animal model of NASH. Most can be categorized as dietary-induced, genetic, and combination models [70]. Some of these models successfully mimicked the early phenotypes of NASH, such as steatohepatitis and hepatic fibrosis [71,72]. The diet-induced mouse model, a methionine- and choline-deficient (MCD) diet-fed model, has been frequently used [73]. The MCD diet induces a decrease in hepatic β-oxidation and the production of VLDL [73]. In addition, a choline-deficient diet impairs hepatic VLDL secretion [74]. These changes lead to the accumulation of intrahepatic lipids and the rapid development of severe and persistent steatohepatitis in 10–14 weeks [75].

However, the MCD diet also has some disadvantages, including severe weight reduction and lack of insulin resistance, as obesity and diabetes are both key etiological factors of NASH [72,76]. The choline-deficient, amino acid-defined (CDAA) diet is another diet commonly used to induce hepatic fibrosis and exerts minimal effects on body weight and glucose metabolism in mouse [77,78] or rat [79]. Many other studies have suggested that dietary lipid conditions, such as high cholesterol, high fat, trans fat, or high fructose, could accelerate NASH formation in rodents [78,80–84]. Therefore, further modification of dietary compositions may offer a valuable approach to induce advanced NASH.

Recently, low-density lipoprotein receptor knockout ($LDLR^{-/-}$) mouse, a well-known animal model of dyslipidemia and atherosclerosis [85,86], was reported to develop NASH-like phenotypes under high cholesterol or high fat dietary conditions [80,83,87–89]. However, 12–24 weeks were required to induce hepatic fibrosis, even with a cholesterol diet [80,83], and there are also no reports on advanced diseases, such as cirrhosis or hepatocellular carcinoma in $LDLR^{-/-}$ mice. In addition, mice with naturally occurring genetic mutations, such as *db/db* mice and *ob/ob* mice, and mice with targeted genetic mutations, such as melanocortin 4 receptor knockout mice and liver-specific phosphatase and tensin homolog deleted from chromosome 10 knockout mice, have been used for the study of NASH, as they have overlapping phenotypes with the risk factors of NASH [70].

A combined model of genetic modification and dietary challenge is theoretically expected to replicate more severe and relevant phenotypes of human NASH and develop form the early to the end stage of the disease [70]. For example, *db/db* mice, a well-known animal model of type 2 diabetes and obesity, showed features of NASH,

including hepatic fibrosis and inflammation, when fed an MCD diet for 4 weeks; however, the development of advanced cirrhosis or HCC by this model is not well characterized [90]. In addition to the model, many other combined models have been reported using mice [91,92] and rats [93].

1.6 Objectives of this research

Overall, given the clinical importance and lack of approved agents for NASH, there is an urgent need for a novel therapeutic agent to reverse or prevent the progression of the disease. The final goal of this research is to provide therapeutic options in the form of pharmacological candidates for the treatment of NASH.

To address the goal, this research was performed in three phases. First, a novel mouse model of NASH using the $LDLR^{-/-}$ mouse fed a modified CDAA diet was developed and comprehensively profiled to investigate whether the model showed appropriate pathophysiological features that overlap with NASH (Chapter 2). Second, the mouse model was pharmacologically benchmarked by using clinically-proven drugs (Chapter 3). As pioglitazone was reported to improve the liver histology in patients with NASH [63], the effect of the drug on hepatic injury, steatosis, and fibrosis in the mouse model was examined. Finally, the therapeutic potential of novel agents for the treatment of NASH was evaluated (Chapter 4). A drug repositioning approach, a process of converting marketed drugs to new indications, was used in this research to allow the administration of drugs to patients with NASH over a shorter timeframe. Similar to pioglitazone, dipeptidyl peptidase-4 (DPP-4) inhibitors, which have been prescribed for type 2 diabetes, were also reported to improve NAFLD in clinic [94–96]. Therefore, the

concomitant therapy of pioglitazone and alogliptin, a DPP-4 inhibitor, was compared with the relevant monotherapies using the developed mouse model.

Chapter 2

Comprehensive profiling of a novel mouse model of NASH

2.1 Objectives

The main purpose of this study was to establish a novel mouse model of NASH which shows more severe and relevant phenotypes of human disease compared with those reported before. $LDLR^{-/-}$ mice under the modified CDAA diet was comprehensively profiled over 1 year to investigate whether this model developed hepatic steatosis, cirrhosis, or HCC in this study. $LDLR^{-/-}$ mice which has the background of dyslipidemia were selected since they were reported to develop NASH-like phenotypes under high-cholesterol or high-fat diet condition [80,83,87–89]. CDAA diet was modified by addition of 1% cholesterol since it would be expected to induce severe NASH-like phenotype without showing body weight reduction [77,78,83].

The additional purpose of this study was to confirm that the mouse model shows relevant phenotypes of NASH independently of obesity. Some studies in Asian countries demonstrated that NAFLD could be also found in subjects without obesity (body mass index < 25 kg/m^2) although obese is generally associated with the development and progression of NAFLD [97,98]. In fact, 15% to 21% of Asian subjects with NAFLD were reported to be non-obese [98]. In addition, another report demonstrated that NAFLD patients without obesity were at a higher risk for diabetes, hypertension, and MS than those with obesity [97]. A mouse model of NASH without obesity is required as well as that with obesity to develop novel agents especially for NASH patients without obesity. Therefore, we investigated whether $LDLR^{-/-}$ mice with the modified CDAA showed relevant phenotypes of NASH independently of obesity in this study.

2.2 Materials and methods

2.2.1 Animal

Homozygous LDLR$^{-/-}$ mice were originally obtained from Jackson Laboratories (Bar Harbor, ME, U.S.A.), and a colony was maintained in Takeda Rabics (Osaka, Japan). Six-week-old male LDLR$^{-/-}$ mice were used in this study. After an acclimation period for a few weeks under normal chow diet (CE-2, Clea Japan, Tokyo, Japan), animals were fed with chow or modified CDAA diet (A08111307, Research Diets, New Brunswick, NJ, U.S.A.). The components of the modified CDAA diet are described in Table 1. All animal experiments were carried out according to the guidelines of the Institutional Animal Care and Use Committee in Takeda Pharmaceutical Company Ltd (Kanagawa, Japan).

Table 1 Components of the modified CDAA diet

Total (g)	864.75
Total L-amino acids (g)	164.5
(L-Methionine (g))	(1.5)
Corn Starch (g)	274
Maltodextrin10 (g)	125
Cellulose (g)	50
Corn oil (g)	25
Palm Oil (g)	150
Mineral Mix S10026B (g)	50
Sodium Bicarbonate (g)	7.5
Vitamin Mix V10001 (g)	10
Choline Bitrartrate (g)	0
Cholesterol (g)	8.7
FD&C Blue Dye #1 (g)	0.05
Protein (w/w%(kcal%))	19 (17)
Carbohydrate (w/w%(kcal%))	47 (42)
Fat (w/w%(kcal%))	20 (41)
Kcal/g	4.5

Cholesterol was added as 1 w/w%. Fat weight was increased up to 41 kcal% and fat origin was changed to palm oil as palmitate-rich oil. Choline was deficient and methionine was restricted.

2.2.2 Sample collection

Body weight was monitored once weekly throughout the experiments. Blood samples were collected from tail vein under a non-fasted state. After the diet feeding periods, the mice were anesthetized with isoflurane and euthanized by over-bleeding from the abdominal aorta, and thoracic and abdominal organs were examined macroscopically. The liver was collected and weighed. Liver samples were kept in 10% neutral buffered formalin for histology or in RNAlater (Life Technologies, Carlsbad, CA, U.S.A.) for RNA analysis. The sample sets of experimental groups are described in Table 2.

Table 2 Liver samples from each experiment to develop a mouse model of NASH-associated hepatic fibrosis and HCC using genetic modification and dietary challenge

Diet	Experiment number	Diet feeding period	Liver weight measurement	Hematoxylin Eosin stain	Sirius red stain	Fibrosis area measurement	mRNA measurement	Immuno-histochemistry
mCDAA	Experiment-1	1W	4	4	4	4	4	N.D.
		4W	12	12	12	12	12	N.D.
		8W	10	10	10	10	10	3
	Experiment-2	1W	10	10	10	N.D.	N.D.	3
		4W	10	10	N.D.	N.D.	N.D.	3
	Experiment-3	16W	10	10	10	10	10	3
	Experiment-4	24W	4	4	4	N.D.	N.D.	N.D.
		31W	4	4	4	N.D.	N.D.	N.D.
	Experiment-5	39W	5	5	5	N.D.	N.D.	N.D.
		47W	5	5	5	N.D.	N.D.	N.D.
	Experiment-6	24W	6	6	6	N.D.	N.D.	N.D.
		32W	6	6	6	N.D.	N.D.	N.D.
		39W	8	8	8	N.D.	N.D.	N.D.
		47W	7	8	8	N.D.	N.D.	N.D.
Chow	Experiment-1	4W	3	N.D.	N.D.	N.D.	N.D.	N.D.
	Experiment-2	1W	8	N.D.	N.D.	N.D.	N.D.	N.D.
	Experiment-3	16W	8	8	8	7	7	3
	Experiment-6	32W	5	5	5	N.D.	N.D.	N.D.
		39W	6	6	6	N.D.	N.D.	N.D.
		47W	6	6	6	N.D.	N.D.	N.D.
	Experiment-7	32W	4	4	4	N.D.	N.D.	N.D.
		39W	4	4	4	N.D.	N.D.	N.D.
		47W	4	4	4	N.D.	N.D.	N.D.

Liver samples were collected from $LDLR^{-/-}$ mice fed normal chow or a modified choline-deficient, amino acid-defined (mCDAA) diet, weighed, and submitted to histological evaluation, immunohistochemistry, and RNA analysis. N.D.; not determined

2.2.3 Blood biochemistry

Plasma glucose, triglyceride, total cholesterol, high-density lipoprotein (HDL) cholesterol, aspartate aminotransferase (AST), and alanine aminotransferase (ALT) levels were measured using an automatic analyzer (type 7180 HITACHI, Tokyo, Japan). Non-HDL cholesterol was calculated as the difference between total cholesterol and HDL cholesterol.

2.2.4 Measurement of hepatic mRNA level

Total RNA was isolated with RNeasy Mini Kit (Qiagen, Valencia, CA, U.S.A.) from the RNAlater-fixed liver samples. Reverse transcription into cDNA was carried out using a High Capacity cDNA Reverse Transcription Kit (Life Technologies). Gene expression was quantified by *Taq*Man real-time PCR using the ABI prism 7900HT Sequence Detection system (Life Technologies). Gene expression was normalized by glyceraldehyde 3-phosphate dehydrogenase expression.

2.2.5 Histological evaluation

Livers were fixed in formalin, embedded in paraffin, sectioned, stained with hematoxylin-eosin and Sirius red and examined microscopically by a certificated pathologist. Histopathological evaluation on hepatocellular proliferative lesions was carried out according to the International Harmonization of Nomenclature and Diagnostic Criteria [99]. Briefly, the diagnostic criteria were as follows: Hepatocellular

hyperplasia: the lesions spanning several hepatic lobules in which portal triads and central veins are present, Hepatocellular adenoma, lesions that are greater than several lobules and have no portal triads and central veins, HCC, neoplastic hepatocytes forming trabeculae of multiple cell layers are evident. The findings and diagnosis were reviewed by another certified pathologist to improve the quality of the pathology data. For quantitative analysis of Sirius red-positive fibrosis areas, four bright field images of a stained section of left lateral lobe for each animal from weeks 1 to 16 were captured using a BX53 microscope and a DP-20 digital camera (both Olympus, Tokyo, Japan) at 113–fold magnification. We captured four digital pictures which excluded existing connective tissue areas around large vasculature and bile ducts as much as possible. Fibrosis areas were measured using the WinROOF image analyzing system (Mitani Corp., Tokyo, Japan) and the results were determined as the means of the four fields of each section.

2.2.6 Immunohistochemistry

Immunohistochemical analysis was carried out for animals treated from week 1 to 16 using following the primary antibodies: rat anti-mouse monoclonal antibody for F4/80 as a marker of macrophages (Ready to use; Abcam, Cambridge, UK), goat polyclonal antibody for desmin as a marker of stellate cells (1:100 dilution; Abcam), rabbit polyclonal antibody for MPO as a marker of neutrophils/monocytes (1:50 dilution; Abcam), mouse anti-human monoclonal antibody for α-smooth muscle actin (α-SMA) as a marker of activated stellate cells (1:100 dilution; Dako, Glostrup, Denmark), rabbit monoclonal antibody for Ki-67 as a marker of cellular proliferation

(1:400 dilution, Abcam), and ApopTag peroxidase *in situ* apoptosis detection kit was used for TdT-mediated dUTP nick end labeling (TUNEL) method (Millipore, Billerica, MA, U.S.A.).

2.2.7 Hepatic triglyceride measurement

Liver tissues were homogenized in 3.35% sodium sulfate solution. After extracting lipid with hexane:isopropanol (3:2), samples were dried and redissolved with isopropanol. Triglyceride content was measured by an automatic analyzer.

2.2.8 Statistical analysis

Statistical significance between the normal chow group and the modified CDAA diet group was analyzed with Student's *t*-test or Aspin–Welch test with or without Bonferroni adjustments. Associations between hepatic fibrosis area and hepatic gene expression in the diet-fed mice were measured with Pearson correlation coefficient. *P*-value less than 0.05 was statistically significant. Data was represented as mean ± standard deviation (SD).

2.3 Results

2.3.1 Time-course changes in body weights, liver weights, and plasma parameters

Body weight in the diet-fed mice mildly increased, but was significantly smaller

compared with chow-fed mice between weeks 4 and 31/32 (Figure 1A). Unlike MCD models, continued and severe weight loss could be avoided under modified CDAA diet conditions. Liver weight continued to increase from week 1 and throughout the experimental period (Figure 1B). Epididymal white adipose tissue weights in the modified CDAA diet group were not changed statistically compare to those in the normal chow group (data not shown).

Plasma glucose levels were slightly but significantly lower with modified CDAA diet (Figure 2A). Although the modified CDAA diet contained a high calorie compared to normal chow, insulin resistance were not observed. Plasma triglyceride, total cholesterol, and non-HDL cholesterol levels were significantly increased, in particular, after week 23 (Figure 2B–D), which might be the result of maxed-out accumulation of hepatic lipids although the exact reason was unclear. Plasma AST and ALT levels, as markers of hepatic injury, were dramatically increased by the diet challenges, peaked at week 4 and sustained the high levels thereafter (Figure 2E,F).

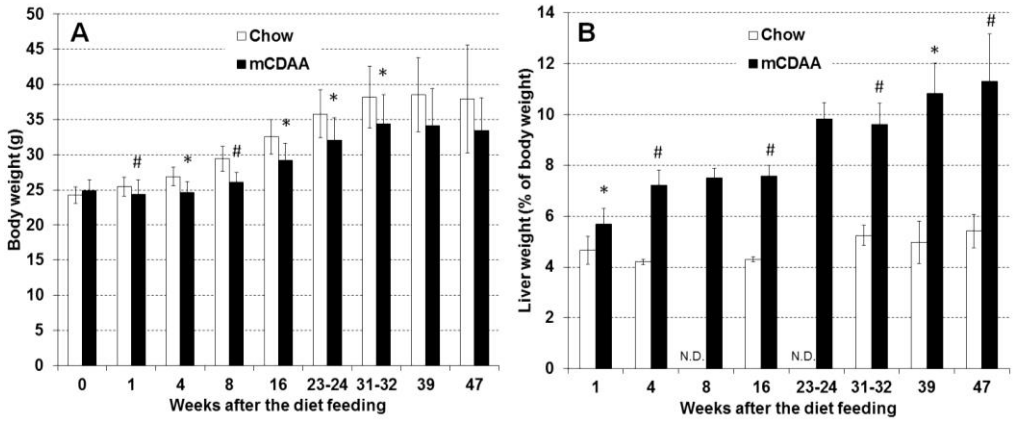

Figure 1 Body weights (A) and liver weights (B) in LDLR$^{-/-}$ mice with or without modified CDAA diet.

Body weights were measured over time from the same individuals (n = 10–56). Liver weights were measured under non-fasted state in each week (n = 3–22). *P < 0.05 vs normal chow control each week by Student's t test with Bonferroni adjustments. $^{\#}P$ < 0.05 vs normal chow control each week by Aspin–Welch test with Bonferroni adjustments. Mean ± SD. N.D., not determined.

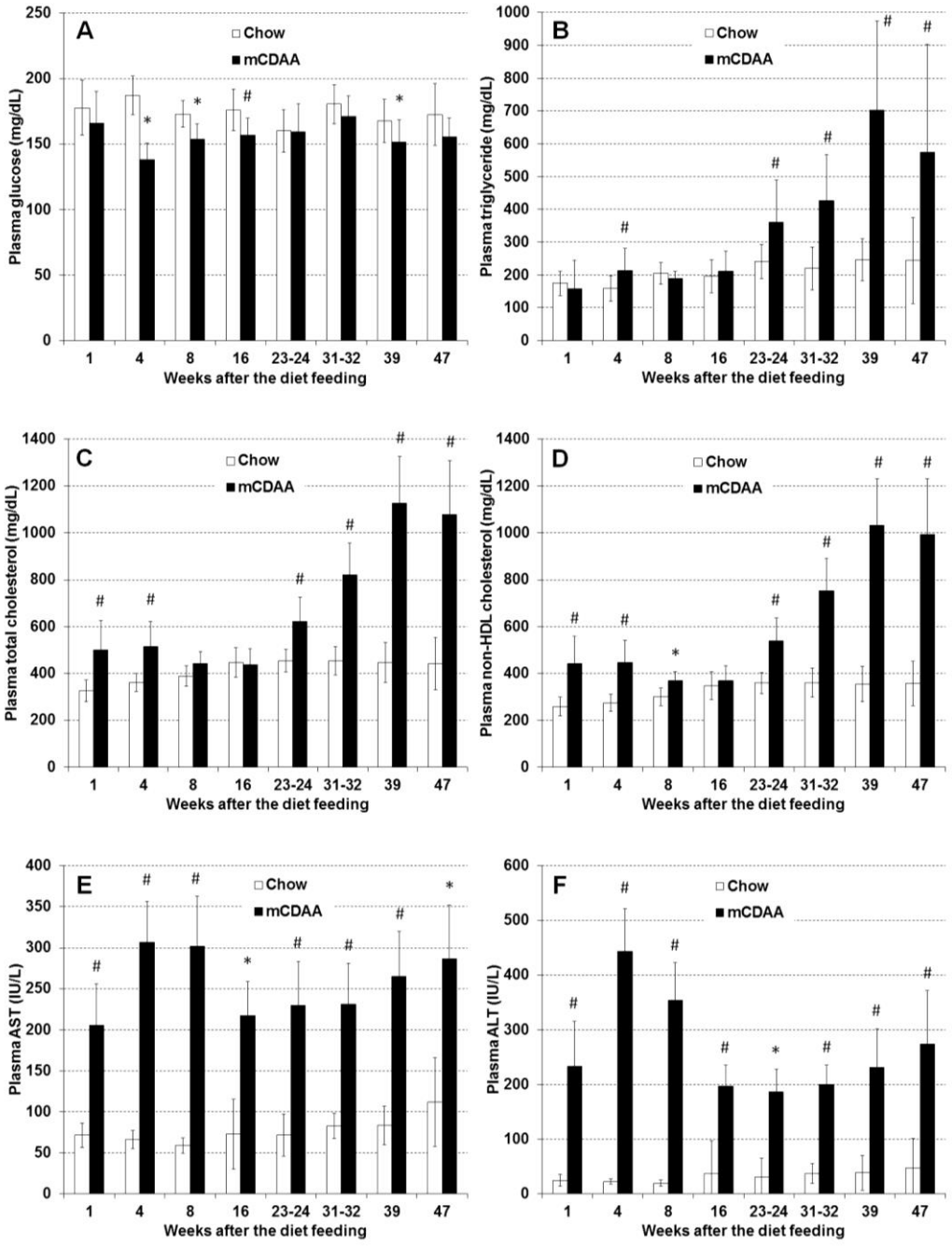

Figure 2 Blood biochemistry in LDLR$^{-/-}$ mice with or without modified CDAA diet.

Blood samples were collected under non-fasted state over time from the same individuals (n = 8–84). Plasma glucose (A), triglyceride (B), total cholesterol (C), non-high-density lipoprotein (non-HDL) cholesterol (D), aspartate aminotransferase

(AST) (E), and alanine aminotransferase (ALT) (F) levels were measured using an automatic analyzer. *P < 0.05 vs normal chow control each week by Student's t-test with Bonferroni adjustments. $^{\#}P$ < 0.05 vs the normal chow control each week by Aspin–Welch test with Bonferroni adjustments. Mean ± SD.

2.3.2 Time-course changes in histopathological and immunohistochemical findings

At week 1, macrovesicular steatosis characterized by hepatocytes with a cytoplasmic single large vacuole and microvesicular steatosis characterized by hepatocytes with foamy appearing cytoplasm were observed around periportal and centrilobular areas, respectively (Figure 3A). The degree of microvesicular steatosis was decreased gradually and disappeared at week 8. In contrast, macrovesicular steatosis continuously progressed and was observed in almost all hepatocytes, including those in the centrilobular area at week 8. It was slightly attenuated at week 16 (Figure 3A–D). As with the histological findings, hepatic triglyceride levels were massively increased from week 1 (Figure 4). Hepatic fibrosis was observed from week 4 and was exacerbated with time (Figure 3F–I), and advanced hepatic fibrosis was observed at week 16 (Figure 3I). In the study designed to compare the degree of fibrosis progression between $LDLR^{-/-}$ mice with modified CDAA diet and C57BL/6J mice with the modified CDAA diet, $LDLR^{-/-}$ mice showed more prominent fibrosis than C57BL/6J mice in week 12 (Figure 5). Although hepatocellular ballooning is one of the characteristic findings of NASH in human [6,100], the mice did not show hepatocellular ballooning throughout the experiments.

Inflammatory cell infiltration was observed at week 1, and its severity increased by week 4 and remained constant thereafter (Figure 3K–N). Infiltrated cells consisted mainly of F4/80-positive macrophages and MPO-positive neutrophils and monocytes (Figure 6), and some of the cells showed the immunoreactivity for Ki-67, indicating the increased proliferative activity of these cells (Figure 6).

Single cell necrosis of the hepatocytes was observed from week 1 throughout the

experiments (Figure 3M, N); however, TUNEL staining showed that most of the apoptotic cells were inflammatory cells but not hepatocytes (Figure 6). In addition, Ki-67-positive hepatocytes were noted at week 1, and increased until week 4 and remained constant thereafter (Figure 6).

Preceding the development of fibrosis, populations of both desmin-positive hepatic stellate cells and α-SMA-positive activated stellate cells were increased time-dependently from week 1 (Figure 6). Increased desmin-positive cells were mainly seen around inflammatory cell foci, and in these areas, Ki-67-positive spindle cells, possibly proliferating stellate cells, were also observed (Figure 6).

Macroscopically, rough surface and multiple nodules were observed in the liver from week 24, and were apparent with time (Figure 7). Microscopically, multiple hepatocellular hyperplasia was observed from week 24 (Figure 8A). The incidence of hyperplasia was increased at weeks 31–32 and was almost 100% thereafter (Table 3). Hepatocellular adenomas developed at weeks 31–32 (Figure 8B, C) and the incidence increased over time to 9 of 13 mice (69%) and 11 of 13 mice (85%) at weeks 39 and 47, respectively (Table 3). Hepatocellular carcinoma was observed in 2 of 13 mice fed modified CDAA (15%) at week 39 (Figure 8D, E); however, the incidence was not increased at week 47 (Table 3).

In the chow diet-fed group, microvesicular steatosis and inflammatory cell infiltration was observed after weeks 32 and 39, respectively. One mice developed hepatocellular adenoma at week 39 in this group; however, neither hyperplasia nor hepatocellular carcinoma were observed throughout the experiment (Table 3).

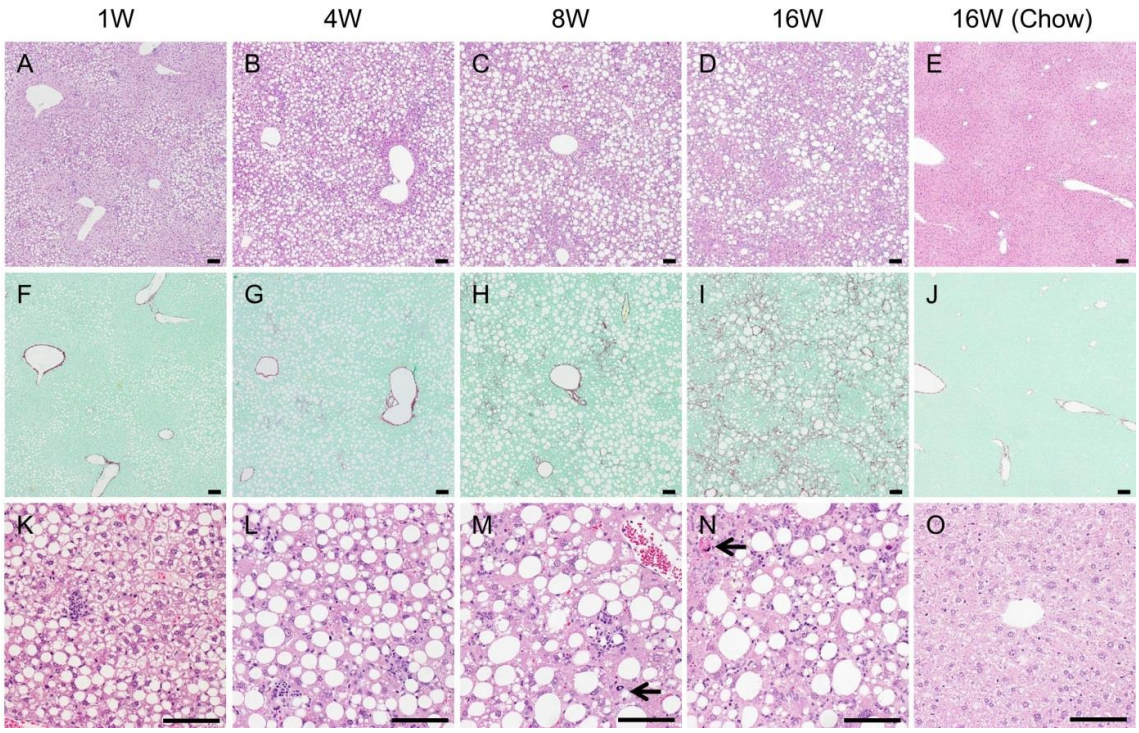

Figure 3 Histopathological features of liver in LDLR$^{-/-}$ mice with or without modified CDAA diet.

(A–E, K–O), hematoxylin-eosin stain; (F–J) Sirius red stain. (A) Macrovesicular and microvesicular steatosis were observed at week 1 (1W) around periportal and centrilobular areas, respectively. (B–D) Macrovesicular steatosis was exacerbated with time and was observed in almost all hepatocytes including the centrilobular area at week 8, but was slightly decreased at week 16. (F–I) Fibrosis was observed from week 4 and exacerbated with time. (K–N) Inflammatory cell infiltration, mainly composed of macrophages and neutrophils, was observed from week 1, increased and kept the same degree from week 4 and thereafter. Single cell necrosis of hepatocytes (arrows) was also seen in all experiment period. (E, J, O) No histopathological abnormalities were observed in the liver of mice fed with normal chow diet. Bar = 100 μm.

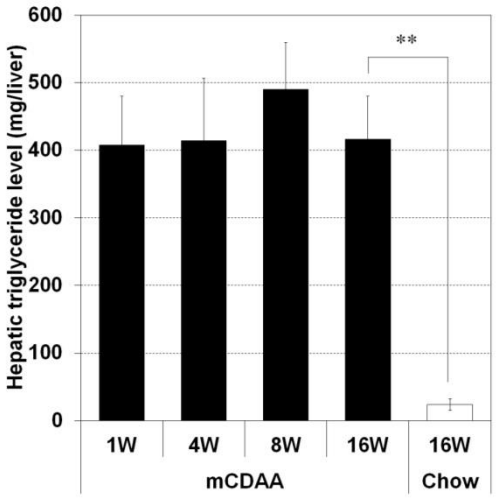

Figure 4 Hepatic triglyceride level in LDLR$^{-/-}$ mice with or without modified CDAA diet.

Liver tissues were homogenized in 3.35% sodium sulfate solution. After extracting lipid with hexane:isopropanol (3:2), samples were dried and redissolved with isopropanol. Triglyceride content was measured by an automatic analyzer. The results were determined as the triglyceride content in each whole liver (n = 4–12). $^{\#}P < 0.05$ vs the normal chow control at week 16 by Aspin–Welch test. Mean ± SD.

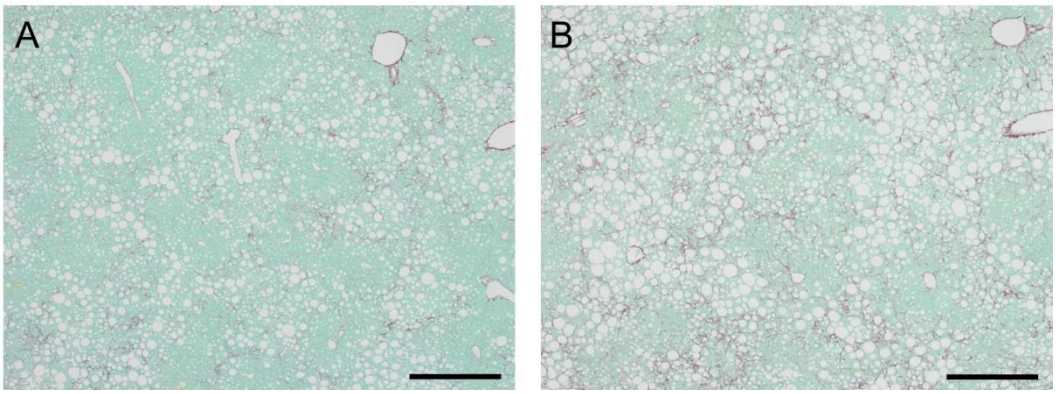

Figure 5　Comparison of histopathological features of the liver in LDLR$^{-/-}$ mice and C57BL/6J mice with modified CDAA diet.

Nine-week-old, male LDLR$^{-/-}$ mice and age-matched C57BL/6J mice were fed a mCDAA diet for 12 weeks (n = 8). The LDLR$^{-/-}$ mice showed more prominent fibrosis than C57BL/6J mice. Typical images of hepatic fibrosis stained with Sirius red in C57BL/6J mice (A) and LDLR$^{-/-}$ mice (B). Bar = 500 μm.

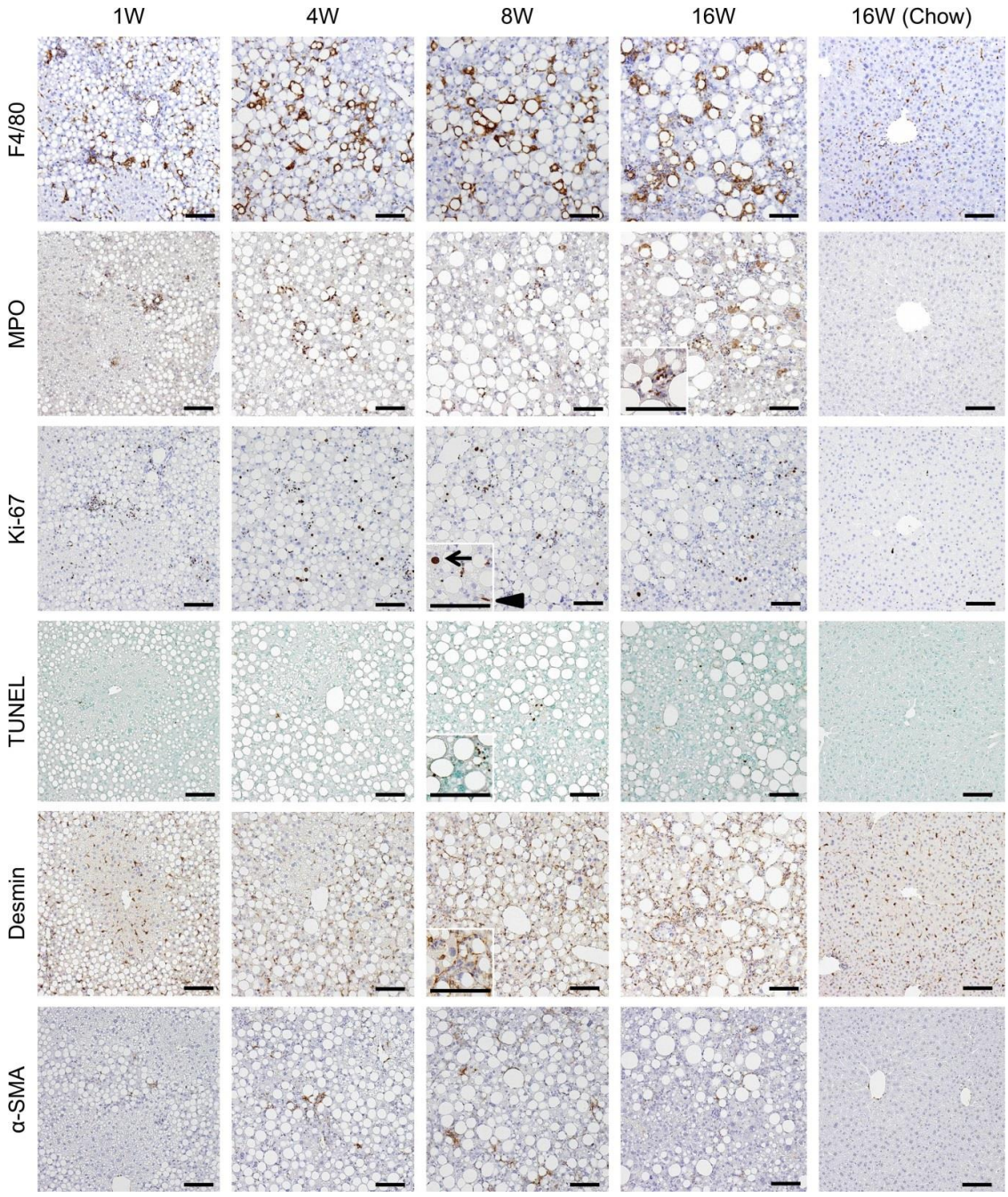

Figure 6 Immunohistological features of liver in LDLR$^{-/-}$ mice with or without modified CDAA diet.

F4/80-positive macrophages, myeloperoxidase (MPO)-positive monocytes and neutrophils (inset), and Ki-67-positive proliferating cells were noted at week 1 (1W); the degree increased by week 4 and was maintained thereafter. Most Ki-67-positive

cells were hepatocytes (arrow), however, some spindle cells, possibly hepatic stellate cells (arrowhead), and inflammatory cells were also positively immunostained for Ki-67. Some terminal deoxynucleotidyl transferase dUTP nick end labeling (TUNEL)-positive cells were also observed and most of these cells were mixed inflammatory cells. Desmin-positive hepatic stellate cells and α-smooth muscle actin (α-SMA)-positive activated stellate cells appeared at week 1 and increased with time. Desmin-positive hepatic stellate cells were observed around inflammatory foci (inset). α-SMA-positive cells were slightly decreased at week 16. Bar = 100 μm.

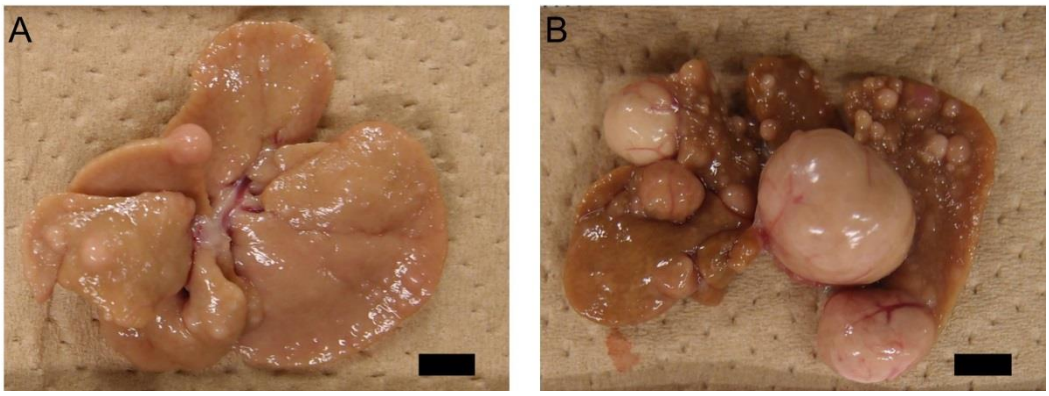

Figure 7 Representative macroscopic features of liver in the LDLR$^{-/-}$ mice with modified CDAA diet.

(A) Multiple white nodules were noted at week 32. (B) Gross lesions were more apparent at week 39. Bar = 5 mm.

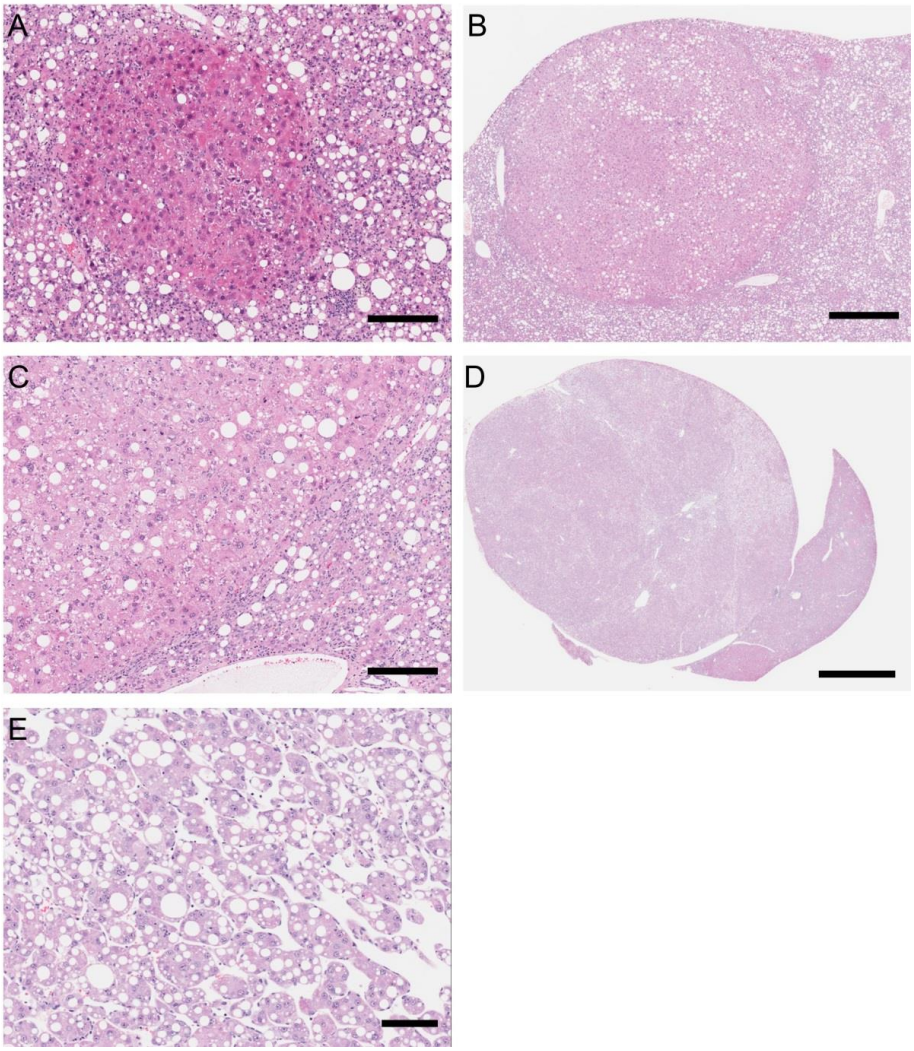

Figure 8 Representative microscopic features of neoplastic lesions of liver in LDLR$^{-/-}$ mice with modified CDAA diet.

Hematoxylin–eosin stain. (A) Hepatocellular hyperplasia was observed at week 24. The lesion spanned several hepatic lobules. Bar = 200 μm. (B) Hepatocellular adenoma was obserbed at week 32. The lesion was larger than several hepatic lobules. Bar = 1 mm. (C) No portal triads were observed in the lesion. High magnification of (B). Bar = 200 μm. (D) Hepatocellular carcinoma was observed at week 39. Bar = 3 mm. (E) Hepatocytes forming trabeculae of mutiple cell layers was noted. High magnification of (D). Bar = 100 μm.

Table 3 Prevalence of histological features in LDLR$^{-/-}$ mice with or without modified CDAA diet.

Duration of chow feeding (week)		24	32	39	47
Animal number (n)		0	9	10	10
Hepatocellular vacuolation, centrilobular	Minimal	N.D.	2 (22%)	3 (30%)	2 (20%)
	Mild	N.D.	5 (56%)	6 (60%)	3 (30%)
	Moderate	N.D.	0 (0%)	1 (10%)	2 (20%)
Single cell necrosis, hepatocyte	Minimal	N.D.	0 (0%)	4 (40%)	3 (30%)
Inflammatory cell infiltration	Minimal	N.D.	0 (0%)	4 (40%)	3 (30%)
Fibrosis	Minimal	N.D.	0 (0%)	0 (0%)	0 (0%)
Hepatocellular adenoma	Present	N.D.	0 (0%)	1 (10%)	0 (0%)

Duration of mCDAA feeding (week)		24	31~32	39	47
Animal number (n)		10	10	13	13
Hepatocellular vacuolation, large	Mild	0 (0%)	0 (0%)	1 (8%)	2 (15%)
	Moderate	10 (100%)	10 (100%)	12 (92%)	11 (85%)
Single cell necrosis, hepatocyte	Minimal	10 (100%)	10 (100%)	13 (100%)	13 (100%)
Inflammatory cell infiltration	Mild	10 (100%)	10 (100%)	13 (100%)	13 (100%)
Fibrosis	Moderate	10 (100%)	10 (100%)	13 (100%)	13 (100%)
Hepatocellular hyperplasia, multiple	Present	6 (60%)	10 (100%)	12 (92%)	13 (100%)
Hepatocellular adenoma	Present	0 (%)	3 (30%)	9 (69%)	11 (85%)
Hepatocellular carcinoma in adenoma	Present	0 (%)	0 (0%)	2 (15%)	0 (0%)

Histological features were graded as minimal, mild, and moderate. N.D., not determined

2.3.3 Hepatic gene expression and fibrosis area

In parallel with inflammatory cell infiltration into the liver, hepatic gene expression of TNF-α, IL-1β, and TGF-β mRNA was increased at week 1 (Figure 9A–C). Although there was large variability of α-SMA mRNA expression, perhaps due to the differences in existing vasculatures, significant increases in expression levels of α-SMA mRNA were observed at week 16 (Figure 9D). Expression of fibrosis-related genes such as collagen-1, tissue inhibitor of metalloproteinase 1 (TIMP-1), and osteopontin were gradually increased after week 4 and significantly elevated at week 16 (Figure 9E–G). Matrix metalloproteinase-9 (MMP-9) expression stayed high after the diet initiation (Figure 9H).

Hepatic fibrosis area measured by digital morphometric analysis was increased from week 4 (Figure 10). Interestingly, expression levels of not only collagen-1 and α-SMA but also TIMP-1 and osteopontin mRNA were strongly related to the fibrosis area (Table 4). Hepatic gene expression of IL-1β was significantly associated with hepatic fibrosis area, however, those of TNF-α or TGF-β levels did not correlated with fibrosis area (Table 4).

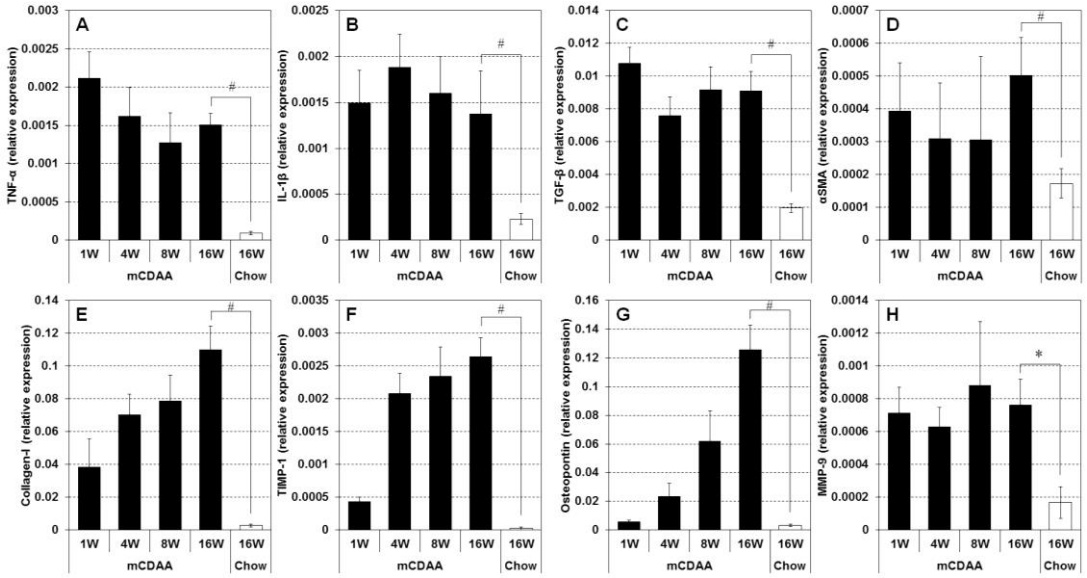

Figure 9 Expression levels of hepatic mRNA in LDLR$^{-/-}$ mice fed modified CDAA diet or chow.

RNAlater-rinsed samples were collected from left lateral lobe under non-fasted state. Gene expression was quantified by *Taq*Man real-time polymerase chain reaction using the ABI prism 7900HT Sequence Detection system. Gene expression was normalized by glyceraldehyde 3-phosphate dehydrogenase (GAPDH) expression. (n = 4–12) *$P < 0.05$ vs normal chow control at week 16 by Student's *t*-test. $^{\#}P < 0.05$ vs normal chow control at week 16 by Aspin–Welch test. Mean ± SD. TNF-α, tumor necrosis factor-α; IL-1β, interleukin-1β; TGF-β, transforming growth factor-β; α-SMA, α-smooth muscle actin; TIMP-1, tissue inhibitor of metalloproteinase 1; MMP-9, matrix metalloproteinase-9.

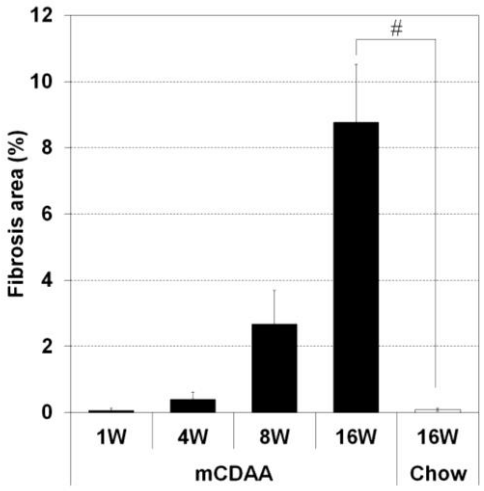

Figure 10　Hepatic fibrosis area in LDLR$^{-/-}$ mice fed modified CDAA diet or chow.

Images in Sirius red-stained sections in each week were captured and fibrosis area was quantified by using the WinROOF image analyzing system (n = 4–12). $^{\#}P < 0.05$ vs normal chow–control at week 16 by Aspin–Welch test. Mean ± SD.

Table 4 Associations between hepatic fibrosis area and hepatic gene expression in LDLR$^{-/-}$ mice fed modified CDAA diet.

Items (mRNA relateive expression)	P values
TNF-α	0.3178
IL-1β	0.0211
TGF-β	0.3599
α-SMA	0.0160
Collagen-I	<0.0001
TIMP-1	0.0007
Osteopontin	<0.0001
MMP-9	0.4339

Associations between hepatic fibrosis area (%) and hepatic gene expression were measured with the Pearson's correlation coefficient (n = 36). $P < 0.05$ was statistically significant. TNF-α, tumor necrosis factor-α; IL-1β, interleukin-1β; TGF-β, transforming growth factor-β; α-SMA, α-smooth muscle actin; TIMP-1, tissue inhibitor of metalloproteinase 1; MMP-9, matrix metalloproteinase-9.

2.4 Discussion

LDLR$^{-/-}$ mouse has been recently introduced as a useful animal model for NASH [87,88]. Although high-fat and/or high-cholesterol condition induced fibrosis formation in LDLR$^{-/-}$ mice [80,83,87–89], there is no report on NASH-associated advanced stages such as cirrhosis and HCC, in the LDLR$^{-/-}$ mouse. The CDAA diet is another well-known NASH-inducible diet without weight loss [78,79]. Therefore, we attempted to combine depletion of LDLR and CDAA diet containing high-fat, high-cholesterol and found this novel rodent model developed end stage diseases, cirrhosis, hepatocellular hyperplasia, adenoma, and carcinoma.

Although obesity is considered as a risk factor for NASH and is generally associated with the disease progression, NASH is also found in lean subjects, especially frequently in Asians [97,98]. Furthermore, leanness in NASH is associated with a high risk for comorbidity of diabetes and hypertension [97]. These results suggest that lean NAFLD patients may have different underlying pathophysiology from obese patients and can be regarded as a subpopulation of NASH. In order to develop a novel drug for the subpopulation, a mouse model of NASH without obesity should be required. In this study, LDLR$^{-/-}$ mice showed relevant phenotypes of NASH independently of obesity and diabetes under the modified CDAA diet. Therefore, this model may represent a subpopulation of lean NASH patients. Furthermore, similar to this model, lean patients may have pathophysiology to accelerate accumulation of intrahepatic lipids, although biochemical and histopathological difference between lean and obese patients has not been reported yet.

The two-hit theory to induce hepatic fibrosis has been proposed and widely

accepted [32,101]. Consistent with the theory, microvesicular steatosis at week 1 and macrovesicular steatosis accompanied with inflammation and hepatic injury was observed prior to fibrosis formation in the current model. A previous report suggested that not only macrophages but also neutrophils played an important role in NASH progression in LDLR$^{-/-}$ mice [50]. MPO-positive neutrophils were also observed in this study and should play a role in inflammatory processes in this model. Given these results, the LDLR$^{-/-}$ mice fed the modified CDAA diet could develop important steatotic and inflammatory features within 4 weeks.

Plasma levels of hepatic transaminases, including AST and ALT, are commonly used biomarkers for hepatic injury. In this study, the LDLR$^{-/-}$ mice fed the modified CDAA diet showed drastic increases in hepatic transaminases, peaked at week 4 and sustained levels with a decreasing trend. In parallel with hepatic transaminases, the mice exhibited continuous progression in hepatic macrovesicular steatosis until week 8 with a slight attenuation at week 16. Similar results were also reported in mice fed a MCD diet [75]. Although the reason for this decreasing trend in hepatic transaminases was uncertain, it may be associated with the decline in newly-formed hepatic injury probably caused by hepatic steatosis. However, given the continued presence of hepatic inflammatory cell infiltration and fibrosis, the declined hepatic injury should be sufficient to maintain the histopathological changes in this model.

Hepatic fibrosis was increased from week 4 to 16 (Figure 3). Compared to periportal fibrosis under high-fat diet condition in LDLR$^{-/-}$ mice [88], the hepatic fibrosis in this model was spread the whole liver at week 8. Although the degree of hepatic fibrosis in this model has not been compared directly in parallel with those in other LDLR$^{-/-}$ models, hepatic fibrosis formation in LDLR$^{-/-}$ mouse with the modified

CDAA diet tends to progress rapidly [80,83,87,88]. Moreover, the $LDLR^{-/-}$ model with modified CDAA diet showed similar or quick fibrosis progression compared to mouse models with MCD [75] or CDAA diets [77,78,102]. Advanced hepatic fibrosis was observed at week 16 (Figure 3I), but unlike humans, bridging fibrosis was not fully developed in this model. Similar to other models [75,78,81,82], bridging fibrosis may be difficult to be reproduced in a diet-induced murine model of NASH. In addition, hepatocellular ballooning, defined as cellular enlargement 1.5–2 times the normal hepatocytes diameter, with rarefied cytoplasm [99], was not observed in this NASH model. Ballooning degeneration is one of the important findings of NASH and reported to indicate poor outcome in humans [5]. However, some NASH models reported previously also did not show hepatocellular ballooning, although they had other appropriate liver pathology for NASH such as steatosis, inflammation, hepatocyte injury and fibrosis [103–105].

The modified CDAA diet contains 1% cholesterol, and it was reported that cholesterol could induce several signals such as free cholesterol-driven oxidative stress or oxysterol-induced hepatocyte apoptosis [106]. Not only choline-deficiency, but also dietary cholesterol, might accelerate inflammatory cell infiltration in the liver, as previously observed [83,89]. Otherwise, as it was suggested that palm oil-derived saturated fat could trigger inflammasomes through toll-like receptor 4 [107] and palmitate but not oleate was reported to induce hepatic injury [108]; palm oil saturated fat in the modified CDAA diet might initiate hepatic injury in this model. Moreover, as it was suggested that saturated fat and cholesterol could accelerate inflammation and hepatic fibrosis [83,89,109]; saturated fat and/or dietary cholesterol in the modified CDAA diet might contribute to the fibrosis formation in this model.

In addition to the dietary lipids, LDLR-deficient condition might be important for hepatic fibrosis progression. It was reported that lipogenic genes were down-regulated by cholesterol diet challenge in wild-type mice [110]. In contrast, lipogenesis-related genes were reported to be up-regulated in LDLR$^{-/-}$ mice even under dietary cholesterol condition, and increase in oxidative stress was observed under the diet condition [83]. Furthermore, inflammatory signals could be activated in LDLR$^{-/-}$ mice with dietary cholesterol and fat, but not in wild-type mice [80]. The combination of these genetic and dietary backgrounds with choline-deficient and methionine-restricted conditions could accelerate NASH progression.

Up-regulation of gene expression of TIMP-1 was observed in parallel with fibrosis formation and elevation of collagen-1 gene in the liver (Figure 9F, Table 4). These data are consistent with the previous report [87,101] and support that not only a transcriptional regulation of collagen-1 but also a fibrolytic modulation is involved in hepatic fibrosis formation [111]. As TIMP-1 expression is correlated more closely with hepatic fibrosis area compared to MMP-9 expression, which peaked at week 1, inhibition of the fibrolytic pathway may play an important role in fibrosis formation in this LDLR$^{-/-}$ model. Interestingly, hepatic osteopontin mRNA was also significantly correlated with hepatic fibrosis area (Figure 9G, Table 4). Osteopontin is known to be up-regulated in the liver of NASH patients and a dietary murine model of NASH [112,113]. As osteopontin itself activates hepatic stellate cells [114], osteopontin may directly contribute to hepatic fibrosis formation.

As hepatocellular hyperplasia is one of the typical findings of cirrhosis [99], the histological features in the mice after week 24 might be classified as cirrhosis. Although the incidence was not high, this LDLR$^{-/-}$ model developed HCC at a relatively early

time point. NASH-associated HCC was observed in wild-type mouse fed CDAA diet at week 84 [77], or in genetic mice such as melanocortin 4 receptor-deficient, phosphatase and tensin homolog-deficient, or galectin-3 knockout mice with normal chow or high-fat diet at approximately 1 year of age [115–118]. Nutritional challenges such as high-cholesterol, high-fructose or high-sucrose diet were alternative options to induce hepatic fibrosis [81,83,84]. However, it took approximately 1 year to observe nodular hyperplasia and tumors [82,110]. Therefore, the combination of genetic modification and CDAA diet including high-fat and high-cholesterol might accelerate carcinogenesis. In the current animal model, hepatocellular hyperplasia and adenoma was observed prior to HCC, sequentially, after week 24.

2.5 Chapter summary

A rodent model of NASH using LDLR$^{-/-}$ mice fed a modified CDAA diet was comprehensively profiled in this study. The mice showed NASH-like phenotypes such as hepatic steatosis, inflammatory cell infiltration, hepatic injury, and hepatic fibrosis. Furthermore, this model showed advanced stages associated with NASH such as hepatocellular hyperplasia, adenoma, and carcinoma. The formation of hepatic fibrosis and hepatocellular carcinoma in this model tended to progress rapidly compared with other reported mouse models. These results suggested that the combination of genetic modification and dietary challenge with choline-deficient and methionine-restricted conditions might accelerate NASH progression and carcinogenesis.

In contrast, the relevant phenotypes of NASH were independent of obesity and diabetes in the mice. These results suggested that this model may represent a subpopulation of lean patients with NASH, which were observed especially among

Asian subjects.

Chapter 3

Pharmacologically benchmarking of a novel mouse model of NASH

3.1 Objectives

In general, an ideal animal model of human disease should show not only similar phenotypes and underlying mechanisms to the disease but also similar responsiveness to known drugs with clinical evidence [119]. Therefore, the pharmacological investigation is also required in order to validate the translatability of the animal model to human.

As described in Chapter 1, pioglitazone improved hepatic histological findings in patients with NASH by decreasing steatosis, ballooning degeneration, lobular inflammation, and fibrosis in a meta-analysis of randomized, placebo-controlled clinical trials [63]. In addition to the clinical evidence, pioglitazone improved hepatic steatosis and fibrosis in a rat model with CDAA diet and directly inhibited activation of rat Kupffer cells and hepatic stellate cells in vitro [120,121].

Angiotensin II type 1 receptor blockers (ARBs), well-known anti-hypertensive drug class, have been tested in clinical trials and preclinical studies for NASH as well as pioglitazone. However, there have been a few conflicting clinical reports on the efficacy of ARBs for NASH. It is a very small non-controlled study, but losartan improved hepatic inflammation and fibrosis, and decreased serum aminotransferase levels in patients with NASH [122]. In contrast, combination therapy with rosiglitazone and losartan conferred no greater benefit than rosiglitazone alone in a randomized, prospective, open-label trial of NASH [123]. Preclinically, in many studies using rodent models of NASH, ARBs have been consistently efficacious. For instance, olmesartan attenuated increases in aminotransferase levels, activation of hepatic stellate cells, oxidative stress, and liver fibrosis in a rat model under MCD diet [124].

As shown in Chapter 2, $LDLR^{-/-}$ mice with modified CDAA diet developed NASH-like phenotypes such as hepatic steatosis inflammatory cell infiltration, hepatic

injury, and hepatic fibrosis. However, the similarity of this model to patients with NASH in the response to drugs was unclear. The purpose of this study was to pharmacologically benchmark and better understand the translatability of a mouse model of NASH, LDLR$^{-/-}$ mice with modified CDAA diet using pioglitazone and candesartan cilexetil, an ARB.

3.2 Materials and methods

3.2.1 Animals

All experimental procedures were approved by the Institutional Animal Care and Use Committee of Takeda Pharmaceutical Company Ltd., which was fully accredited by the Association for Assessment and Accreditation of Laboratory Animal Care International. Breeding pairs of homozygous LDLR$^{-/-}$ mice were obtained from Jackson Laboratories, and a colony was maintained in Takeda Rabics. Seven-week-old male mice were used. After an acclimation period of 2–3 weeks under normal chow diet, animals were fed with normal chow or the modified CDAA diet.

3.2.2 Drugs

Candesartan cilexetil and pioglitazone were synthesized in Takeda Pharmaceutical Company Ltd.

3.2.3 Experimental design

After 1 week under the modified CDAA diet, animals were divided into study groups (week 0). Baseline characteristics of the mice subjected to this study are shown in Table 5. In experiment 1, candesartan cilexetil (3 mg/5 ml/kg, n = 10) was suspended in 0.5% methylcellulose and given orally once daily for 7 weeks. Mice fed with normal chow (n = 4) or the modified CDAA diet (n = 10) in the control groups received 0.5% methylcellulose. In experiment 2, pioglitazone (10 mg/5 ml/kg, n = 10) was suspended in 0.5% methylcellulose and given orally once daily for 7 weeks. Body weight and food intake were monitored once per week throughout the drug treatment period. Blood samples were collected from the tail vein at weeks 3 and 7 under a non-fasted state. On the day after the final dosing, blood samples were collected from abdominal vein under isoflurane anesthesia. Animals were then killed by cervical dislocation and liver tissues, kidney tissues, and epididymal white adipose tissues were harvested.

Table 5 Baseline characteristics of LDLR$^{-/-}$ mice fed normal chow or a modified CDAA diet subjected to the experiments 1 and 2, at week 0.

Parameter	Experiment 1			Experiment 2	
	Chow-Vehicle (n = 4)	mCDAA-Vehicle (n = 10)	mCDAA-Candesartan (n = 10)	mCDAA-Vehicle (n = 10)	mCDAA-Pioglitazone (n = 10)
Body weight (g)	24.5 ± 1.0	24.6 ± 1.4	23.8 ± 1.5	25.5 ± 1.6	25.7 ± 1.2
Glucose (mg/dL)	153.0 ± 1.9	155.0 ± 18.5	150.7 ± 12.4	188.8 ± 16.8	179.3 ± 10.7
Total cholesterol (mg/dL)	353.1 ± 29.9	411.5 ± 65.1	422.9 ± 73.5	510.5 ± 83.0	523.1 ± 137.8
HDL (mg/dL)	89.4 ± 8.4*	63.6 ± 5.2	62.0 ± 7.4	71.5 ± 9.1	72.3 ± 10.3
non-HDL (mg/dL)	263.7 ± 28.8*	347.9 ± 64.8	360.9 ± 69.9	439.0 ± 77.4	450.8 ± 134.7
Triglyceride (mg/dL)	191.4 ± 29.0*	84.3 ± 23.1	85.4 ± 21.4	158.8 ± 47.3	160.9 ± 49.3
AST (IU/L)	68.4 ± 4.0$^{\#}$	205.7 ± 38.7	205.0 ± 25.1	196.3 ± 35.9	195.5 ± 30.2
ALT (IU/L)	28.4 ± 5.7$^{\#}$	231.2 ± 56.0	236.0 ± 46.6	212.8 ± 57.8	220.3 ± 70.5

Experiment 1, mice were fed chow and 0.5% methylcellulose (vehicle), mCDAA and vehicle, or mCDAA and candesartan cilexetil (3 mg /kg) once daily for 7 weeks. Experiment 2, mice were fed mCDAA and vehicle, or mCDAA and pioglitazone (10 mg/kg) once daily for 7 weeks. Blood samples were collected under a non-fasted state. Plasma parameters were measured using an automatic analyzer (n = 4–10). *P < 0.05 vs mCDAA–vehicle group by Student's t-test. $^{\#}P$ < 0.05 vs mCDAA–vehicle group by Aspin–Welch test. HDL, high density lipoprotein; AST, aspartate aminotransferase; ALT, alanine aminotransferase. Mean ± SD.

3.2.4 Blood biochemistry

Blood samples were centrifuged and plasma samples were collected. Glucose, triglyceride, cholesterol, HDL cholesterol, AST, and ALT levels were measured by an automatic analyzer. Non-HDL cholesterol was calculated as the differences between total cholesterol and HDL cholesterol.

3.2.5 Hepatic triglyceride measurement

Liver tissues were homogenized in 3.35% sodium sulfate solution. After extracting lipid with hexane:isopropanol (3:2), samples were dried and redissolved with isopropanol. Triglyceride content was measured by an automatic analyzer.

3.2.6 Quantitative real-time polymerase chain reaction

Total RNA was isolated from liver and kidney with RNeasy Mini Kit. Reverse transcription into cDNA was carried out using a High Capacity cDNA Reverse Transcription Kit. Gene expression was quantified by *Taq*Man real-time polymerase chain reaction using the ABI prism 7900HT Sequence Detection system. Gene expression was normalized by glyceraldehyde 3-phosphate dehydrogenase expression.

3.2.7 Histological analysis

Left lateral lobes of the livers were fixed in 10% formalin neutral buffered solution,

embedded in paraffin, sectioned, and stained with Sirius red. For quantitative analysis of Sirius red-positive fibrosis areas, four bright field images of a stained section for each animal were captured in a blinded manner using a BX53 microscope and a DP-20 digital camera at 113–fold magnification. Fibrosis areas were measured using the WinROOF image analyzing system and expressed as the means of the four fields of each section.

3.2.8 Statistical analysis

The results were presented as mean ± SD. All statistical analyses were undertaken using SAS version 8.2 (SAS Institute, Cary, NC, U.S.A.). Student's *t*-test was used if the variance was homogenous. If the variance was heterogeneous, the Aspin–Welch test was performed. Differences were considered statistically significant at $P < 0.05$.

3.3 Results

3.3.1 Effects on body weight and food intake

Body weight of modified CDAA diet-fed mice was significantly lower compared to chow diet-fed mice (Figure 11A). Food intake of modified CDAA diet-fed mice was also lower than that of normal chow diet-fed mice (Figure 11B). Neither candesartan cilexetil nor pioglitazone had an effect on body weight (Figure 11A, C) or food intake (Figure 11B, D).

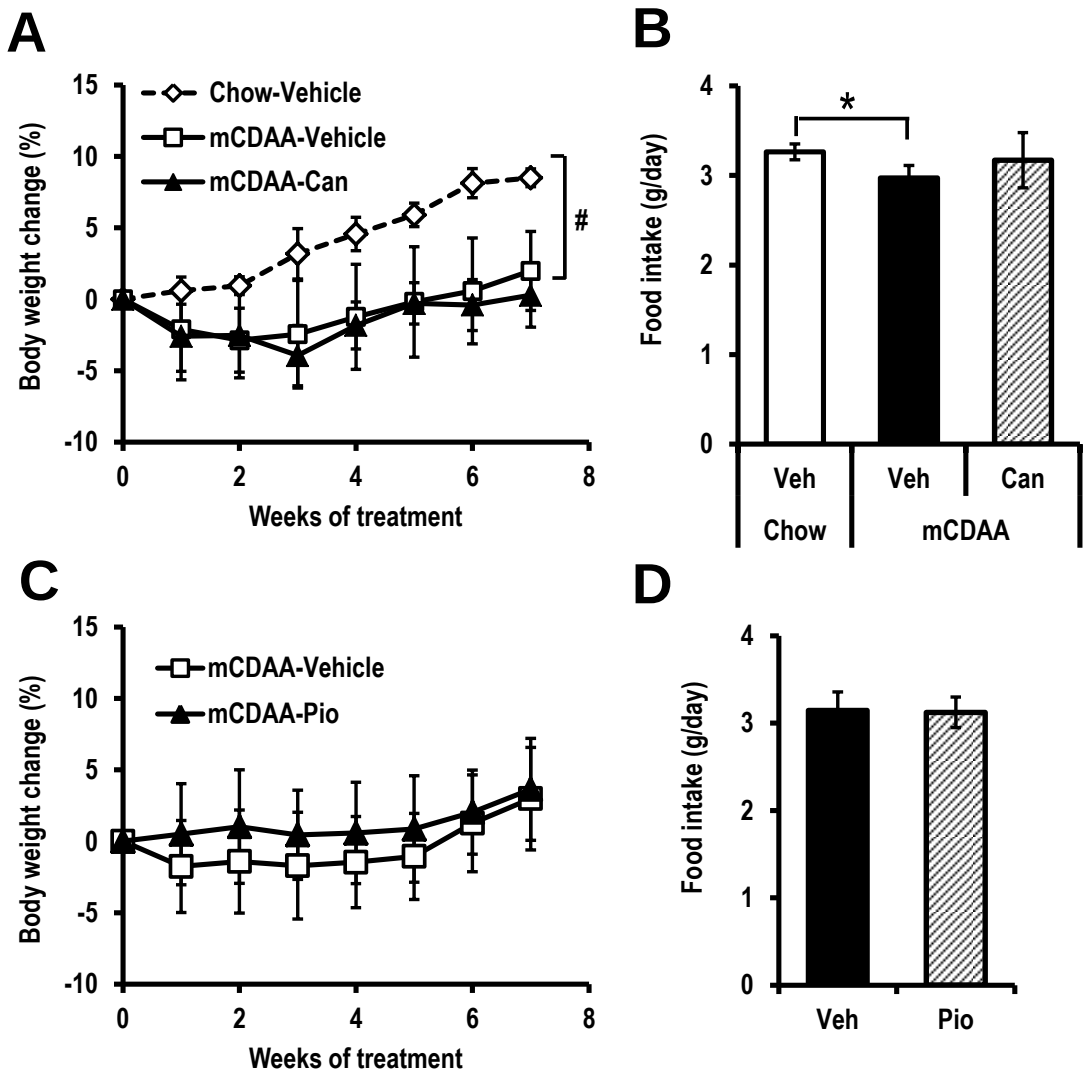

Figure 11 Body weight change and food intake in LDLR$^{-/-}$ mice fed normal chow or a modified CDAA diet.

Mice were treated with 0.5% methylcellulose (vehicle) and candesartan cilexetil (3 mg/kg) (A, B) or pioglitazone (10 mg/kg) (C, D) once daily for 7 weeks. Body weight (A, C) and food intake (B, D) were monitored once per week throughout the drug treatment period (n = 4–10). *P < 0.05 vs mCDAA–vehicle group by Student t-test. $^{\#}P$ < 0.05 vs mCDAA–vehicle group by Aspin–Welch test. Mean ± SD.

3.3.2 Effects on tissue weight and hepatic triglyceride content

Liver weight of modified CDAA diet-fed mice at the end-point increased compared with that of normal chow diet-fed mice (Figure 12A). Treatment with pioglitazone significantly attenuated modified CDAA diet-induced increase in liver weight (Figure 12C), but candesartan cilexetil did not (Figure 12A). The weight of epididymal white adipose tissue, which was surrogate for visceral adipose tissue mass, was not changed by either modified CDAA diet or drug treatment (Figure 12B, D).

Hepatic triglyceride content of modified CDAA diet-fed mice was higher than that of chow diet-fed mice (Figure 13A). Treatment with pioglitazone decreased hepatic triglyceride content (Figure 13B), whereas candesartan cilexetil had no effect (Figure 13A). Representative images of the liver sections stained with hematoxylin–eosin stain in the mice treated with vehicle and pioglitazone are shown in Figure 14.

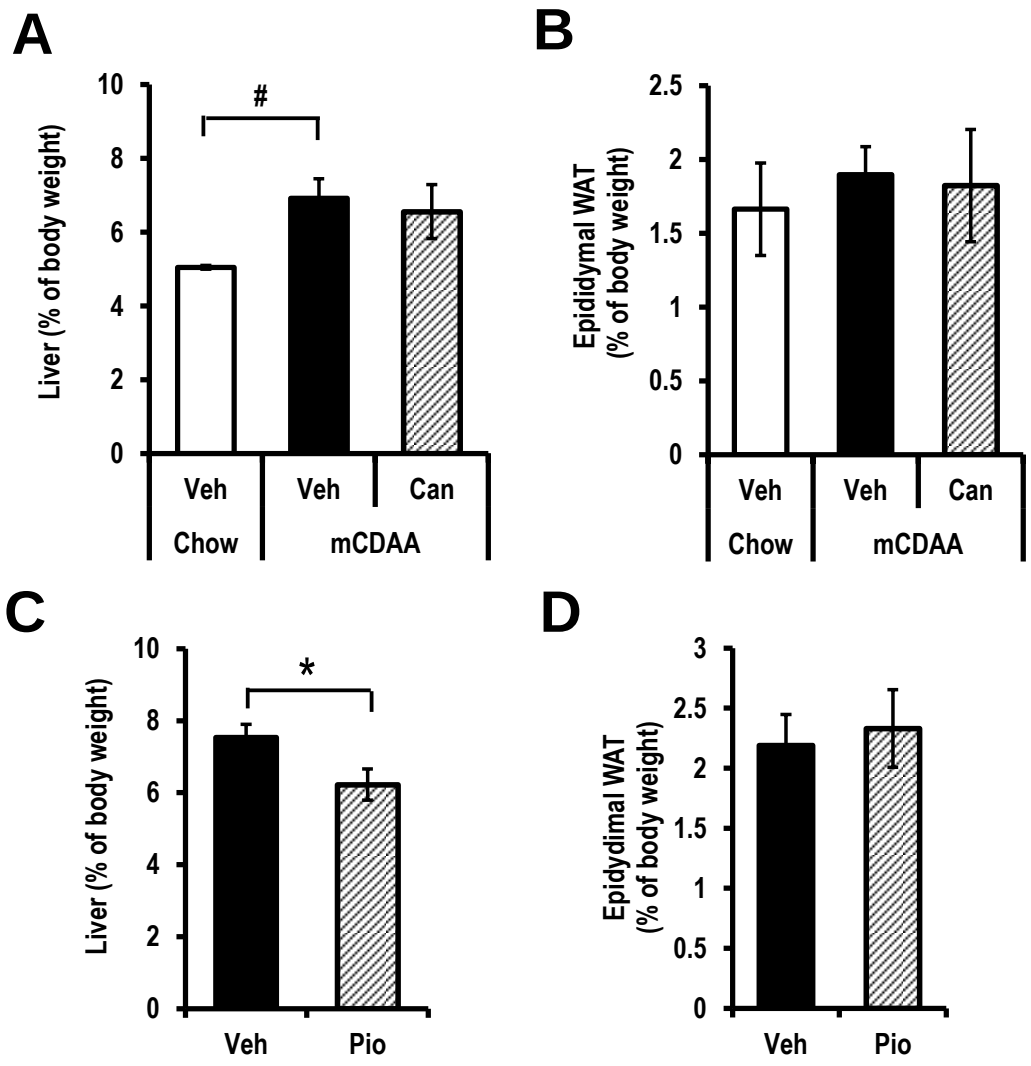

Figure 12 Tissue weight in LDLR$^{-/-}$ mice fed normal chow or a modified CDAA diet at week 7.

Mice were treated with 0.5% methylcellulose (vehicle [Veh]) and candesartan cilexetil (Can; 3 mg/kg) (A, B) or pioglitazone (Pio; 10 mg/kg) (C, D) once daily for 7 weeks. Livers (A, C) and epididymal white adipose tissues (WAT) (B, D) were weighed (n = 4–10). *P < 0.05 vs mCDAA–vehicle group by Student's t-test. $^{\#}P$ < 0.05 vs mCDAA–vehicle group by Aspin–Welch test. Mean ± SD.

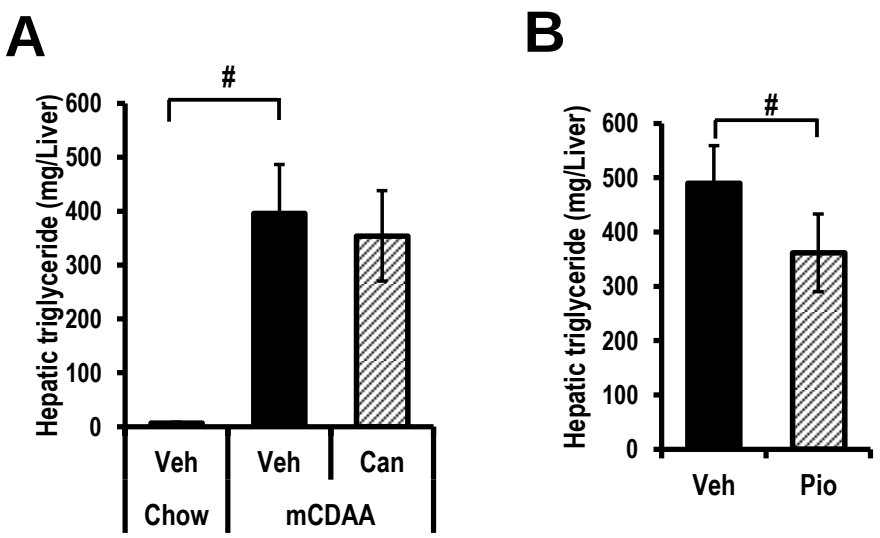

Figure 13 Hepatic triglyceride content in LDLR$^{-/-}$ mice fed normal chow or a modified CDAA diet.

Mice were treated with 0.5% methylcellulose (vehicle [Veh]) and candesartan cilexetil (Can; 3 mg/kg) (A) or pioglitazone (Pio; 10 mg/kg) (B) once daily for 7 weeks. Liver tissues were homogenized in 3.35% sodium sulfate solution. After extracting lipid with hexane:isopropanol (3:2), samples were dried and redissolved with isopropanol. Triglyceride content was measured by an automatic analyzer. The results were determined as the triglyceride content in each whole liver (n = 4–10). *P < 0.05 vs mCDAA–vehicle group by Student's t-test. $^{\#}P$ < 0.05 vs mCDAA–vehicle group by Aspin–Welch test. Mean ± SD.

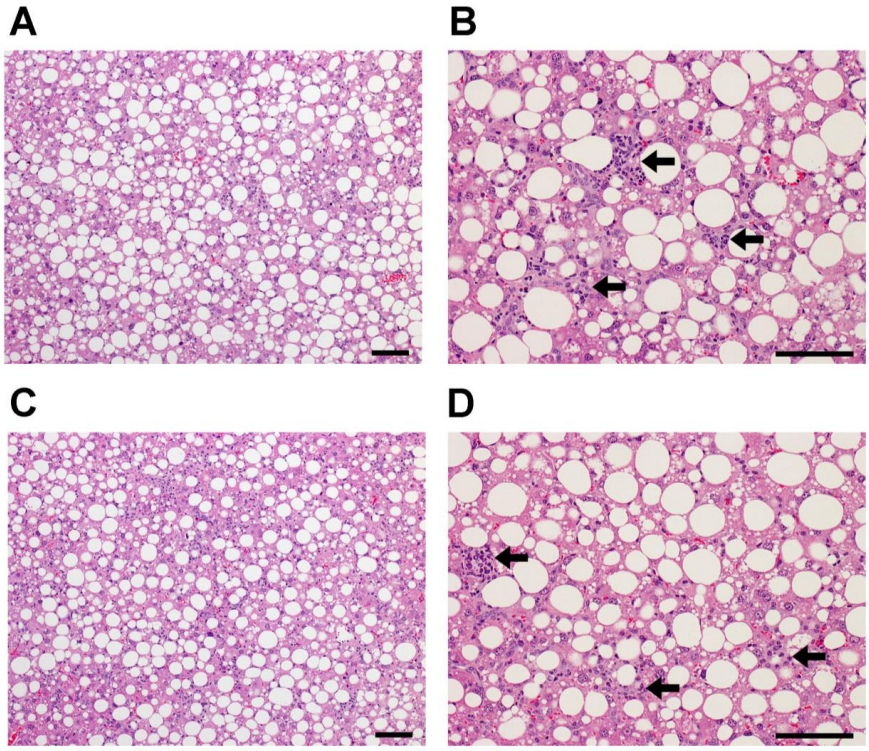

Figure 14 Representative images of liver sections stained with hematoxylin–eosin. Hepatic macrovesicular steatosis and inflammatory cell infiltration (arrows) in modified CDAA diet-fed LDLR$^{-/-}$ mice received 0.5% methylcellulose (A, B) and pioglitazone (C, D). The left lateral lobes of the livers were fixed in 10% formalin neutral buffered solution, embedded in paraffin, sectioned, and stained with hematoxylin–eosin, and examined microscopically. The severity of the macrovesicular steatosis was graded based on the percentage of hepatocytes involved: moderate, >50% of hepatocytes; marked, >70% of hepatocytes. Most animals showed marked macrovesicular steatosis (9 of 10 mice received 0.5% methylcellulose and 7 of 10 mice received pioglitazone). The severity of the inflammatory cell infiltration was graded as mild for all the animals based on the distribution of the foci. As noted above, there were no significant differences in the incidence or severity of macrovesicular steatosis and inflammatory cell infiltration between 0.5% methylcellulose and pioglitazone groups. Bar = 100 μm

3.3.3 Effects on plasma parameters

Plasma ALT levels were elevated with modified CDAA diet through the study period and peaked at week 3 (Figure 15A). Pioglitazone significantly decreased plasma ALT levels at week 3 of treatment, but not at week 7 (Figure 15B). Candesartan had no effect on plasma ALT levels (Figure 15A).

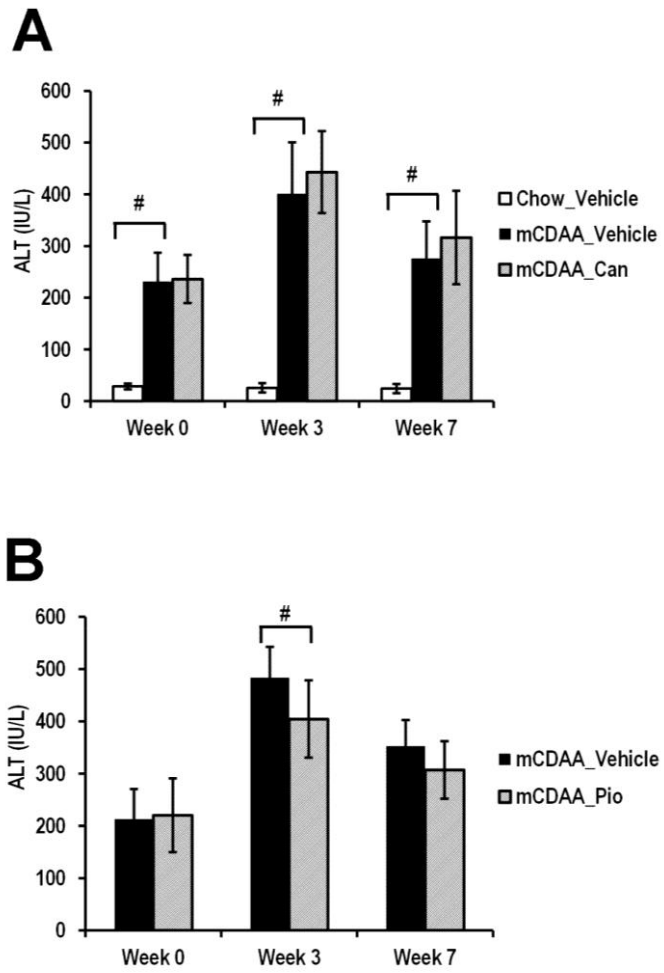

Figure 15 Plasma ALT levels in LDLR$^{-/-}$ mice fed normal chow or a modified CDAA diet.

Mice were treated with 0.5% methylcellulose (vehicle) and candesartan cilexetil (3 mg/kg) (A) or pioglitazone (10 mg/kg) (B) once daily for 7 weeks. Blood samples were collected under a non-fasted state. ALT levels were measured using an automatic analyzer (n = 4–10). *$P < 0.05$ vs mCDAA–vehicle group by Student's *t*-test. $^{\#}P < 0.05$ vs mCDAA–vehicle group by Aspin–Welch test. Mean ± SD.

3.3.4 Effects on hepatic gene expression

Expression of fibrosis-related genes including collagen-1, TGF-β, osteopontin, and TIMP-1 was increased in livers of mice with modified CDAA diet (Figure 16A). Treatment with pioglitazone and candesartan cilexetil decreased collagen-1 gene expression by 43% and 33%, respectively (Figure 16A, B). Treatment with pioglitazone decreased expression of other genes such as TGF-β, osteopontin, and TIMP-1 (Figure 16B), but candesartan cilexetil did not. In addition, pioglitazone suppressed IL-6 gene expression, but not IL-1β (Figure 16A).

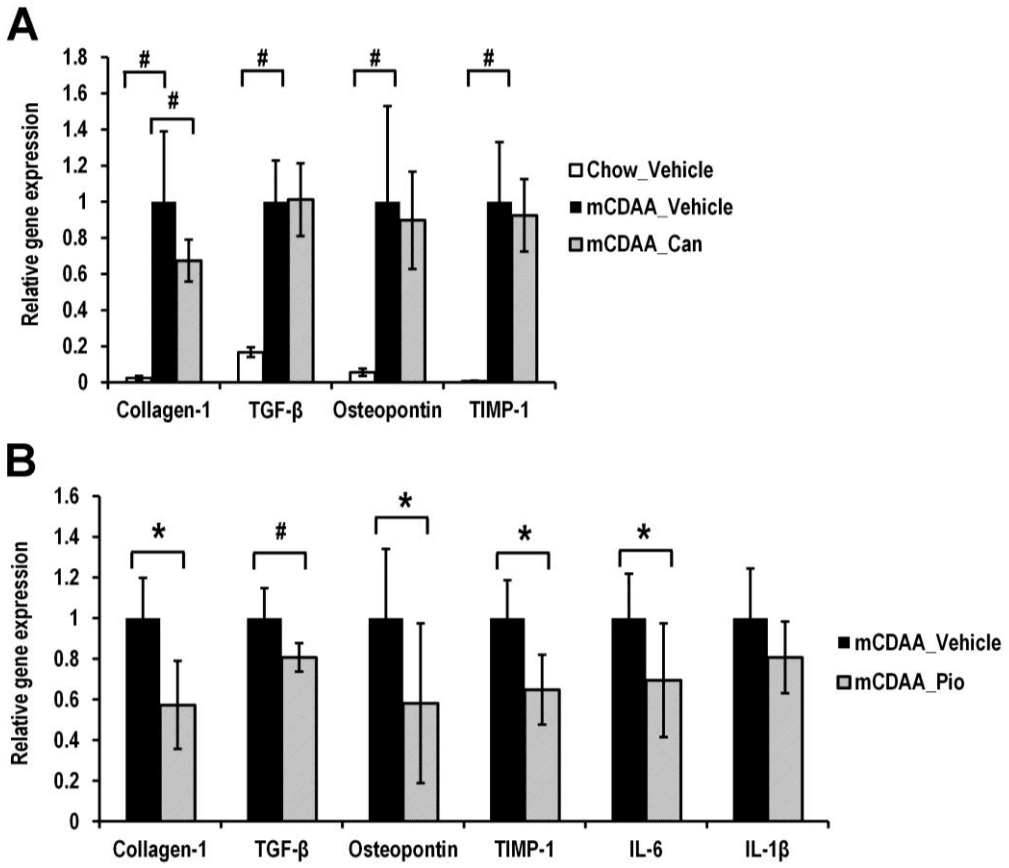

Figure 16 Hepatic gene expression in LDLR$^{-/-}$ mice fed chow or modified CDAA diet.

Mice were treated with candesartan cilexetil (3 mg /kg) (A) or pioglitazone (10 mg /kg) (B) once daily for 7 weeks. RNAlater-rinsed samples were collected from left lateral lobe under non-fasted state. Gene expression was quantified by *Taq*Man real-time polymerase chain reaction using the ABI prism 7900HT Sequence Detection system. Gene expression was normalized by GAPDH expression (n = 4–10). Data are shown by relative gene expression to mCDAA-Vehicle (group). *P < 0.05 vs mCDAA–vehicle group by Student's t-test. $^{\#}P$ < 0.05 vs mCDAA–vehicle group by Aspin–Welch test. Mean ± SD. TGF-β, transforming growth factor-β; TIMP-1, tissue inhibitor of metalloproteinase 1; IL-6, interleukin-6; IL-1β, interleukin-1β.

3.3.5 Effects on renal gene expression

Gene expression of Renin 1 increased in the kidney from candesartan cilexetil-treated mice (data not shown), suggesting that a sufficient dose of candesartan cilexetil was given in this study and target engagement was achieved.

3.3.6 Effects on hepatic fibrosis area

The increase in collagen deposition was observed in the liver from modified CDAA diet-fed mice at week 7, whereas the liver from chow diet-fed mice exhibited a small amount of collagen expression only around the vessels (Figure 17A). Corresponding to the increase in hepatic collagen-1 gene expression, fibrosis areas were remarkably increased in the liver from the modified CDAA diet-fed mice (Figure 17B). Pioglitazone decreased fibrosis area by 49% (Figure 17C), but candesartan cilexetil did not (Figure 17B).

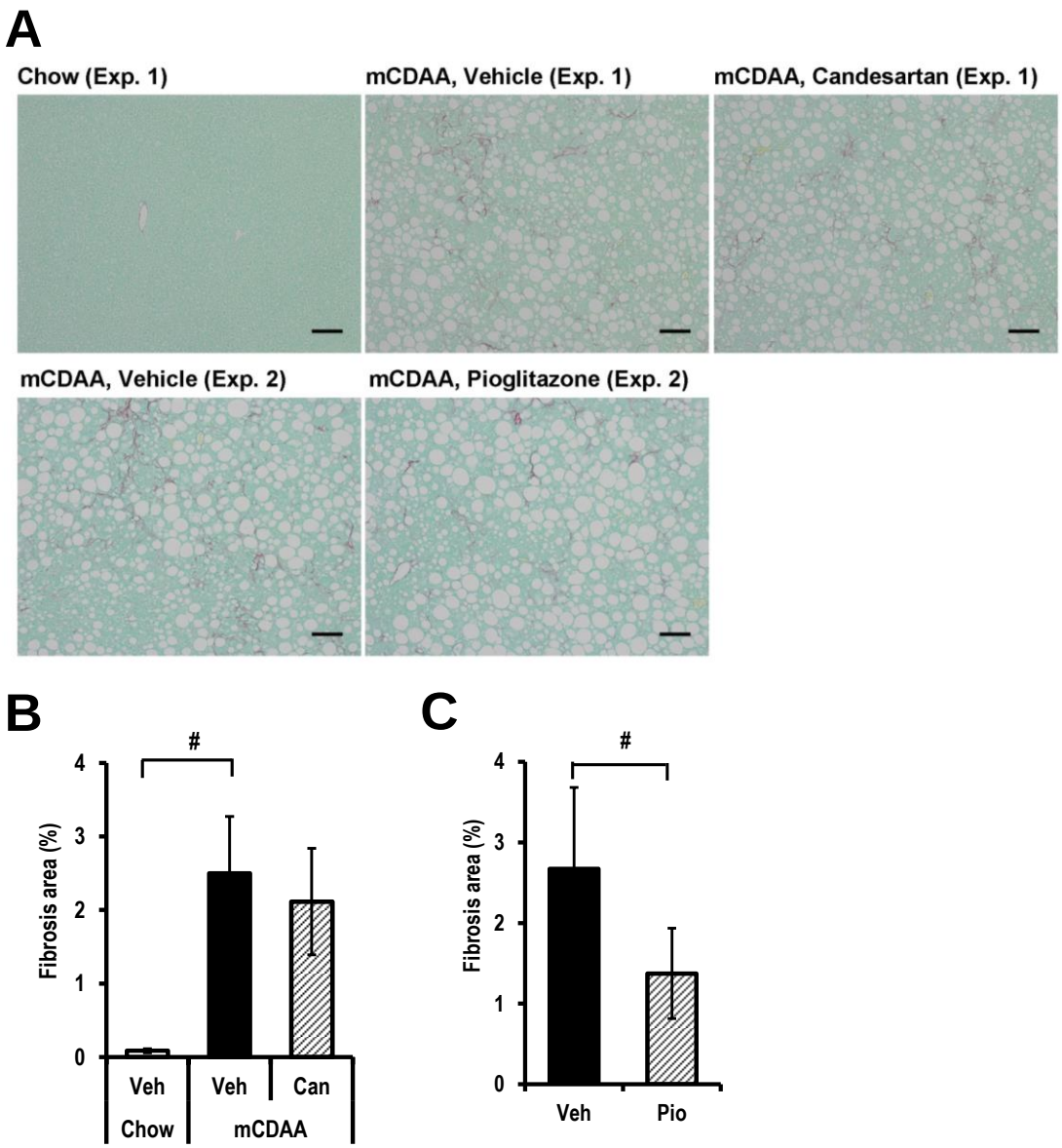

Figure 17 Hepatic fibrosis in LDLR$^{-/-}$ mice fed normal chow or a modified CDAA diet.

Mice were treated with 0.5% methylcellulose (vehicle [Veh]) and candesartan cilexetil (Can; 3 mg/kg) (experiment [Exp.] 1) (A, B) or pioglitazone (Pio; 10 mg/kg) (Exp. 2) (A, C) once daily for 7 weeks. The left lateral lobes of the livers were fixed in 10% formalin neutral buffered solution, embedded in paraffin, sectioned, and stained with Sirius red, and examined microscopically. (A) Representative images of liver sections

stained with Sirius red. Bar = 100 μm. (B, C) Fibrosis areas in Sirius red stained sections were quantified by using the WinROOF image analyzing system and the results were determined as the means of four fields of each section (n = 4–10). $^{\#}P < 0.05$ vs mCDAA–vehicle group by Aspin–Welch test. Mean ± SD.

3.4 Discussion

In order to validate novel pharmacological interventions for NASH, establishing animal models, which reflect the disease pathophysiology, is crucial. As shown in Chapter 2, the modified CDAA diet-fed LDLR$^{-/-}$ mice exhibited phenotypes overlapping with NASH including steatosis, inflammatory cell infiltration, hepatic injury, and fibrosis. In order to further elucidate translatability, this animal model was benchmarked using pioglitazone and candesartan cilexetil that have been tested in clinical studies and whose clinical efficacy is known at some extent.

Pioglitazone, a PPARγ activator, is commonly used for the treatment with type 2 diabetes to improve insulin sensitivity of the liver, muscle, and adipose tissue, promote hepatic fatty acid oxidation and inhibit hepatic lipogenesis [65]. Since MS including type 2 diabetes is a major cause of NASH [2], pioglitazone has been studied in multiple clinical trials for NASH. In a meta-analysis from five independent trials, pioglitazone improved histological findings including hepatocellular ballooning, fibrosis, lobular inflammation, and steatosis [63]. Consistent with the clinical findings, in this study, pioglitazone improved hepatic transaminase activity, hepatic lipid accumulation, inflammatory gene expression, and fibrosis formation in LDLR$^{-/-}$ mice. Although no histological change in infiltration of inflammatory cells was observed in pioglitazone-treated group, pioglitazone might exhibit clearer improvement of inflammation at an earlier time point given the significant reduction in plasma ALT levels at week 4. In previous reports, pioglitazone improved hepatic steatosis and ameliorated hepatic fibrosis in diet-induced models [121,125,126]. Similar to these rodent models of NASH, our model may represent some aspects of hepatic

pathophysiology resembling NASH, in which hepatic lipid metabolism had significant contribution to fibrogenesis.

Candesartan cilexetil, an ARB, is a well-known antihypertensive. Since renin-angiotensin system plays a key role in insulin resistance and activation of hepatic stellate cells [127], blocking renin-angiotensin system seems a reasonable target for the treatment of NASH. ARBs have been tested in a few clinical trials. Losartan showed some benefits such as an improvement of hepatic inflammation and fibrosis in NASH patients in a very small non-controlled study [122]. In a randomized, prospective, open-label trial of NASH, however, losartan in combination with rosiglitazone gave no benefit compared with rosiglitazone alone [123]. Thus, the efficacy of ARBs for NASH is controversial. Larger controlled clinical trials are necessary to determine clinical benefits of ARBs for NASH and a randomized, placebo-controlled trial of losartan has just completed (ClinicalTrials.gov ID: NCT01051219). In contrast, preclinically, there has been reported positive efficacy of ARBs in multiple NASH models. Olmesartan attenuated increases in aminotransferase levels, activation of hepatic stellate cells, oxidative stress, and liver fibrosis in a MCD model [124]. Candesartan cilexetil showed anti-steatotic and anti-inflammatory effects in KK-A^y mice [128], and losartan attenuated hepatic fibrosis induced by CDAA diet in rats with insulin resistance, obesity, and diabetes [129]. In this study, despite a sufficient target engagement, candesartan cilexetil did not inhibit liver injury and prevent from developing steatosis and fibrosis although candesartan cilexetil only suppressed hepatic collagen-1 gene expression.

One of postulated mechanisms of pioglitazone and candesartan cilexetil for NASH is considered to improve insulin sensitivity. In fact, most of animal models that are sensitive to both classes showed insulin resistance. However, $LDLR^{-/-}$ mice that we

used lack at least obesity and hyperglycemia although it is unclear whether the mice exhibited insulin resistance. Activation of renin-angiotensin system is caused by obesity and plays a central role in insulin resistance [130]. Renin-angiotensin system may not be activated and have little contribution to the pathophysiological changes in liver of $LDLR^{-/-}$ mice. Therefore, the potency of pioglitazone and candesartan cilexetil which target insulin sensitivity may be underestimated in this animal model. In other words, pioglitazone would have other mechanisms to improve NASH besides improvement of insulin sensitivity such as direct inhibition of activation of Kupffer cells and hepatic stellate cells as reported before [120,121].

3.5 Chapter summary

In this study, the translatability of the established mouse model to NASH was investigated by a pharmacological approach using two drugs with clinical evidence and different mechanisms. Specifically, the effects of pioglitazone and candesartan cilexetil were examined in $LDLR^{-/-}$ mice with a modified CDAA diet.

Pioglitazone showed anti-fibrotic effects accompanied by improving hepatic transaminase activity and hepatic lipid accumulation in the mice. As the pharmacological effects of pioglitazone in this model were similar to those reported in NASH patients, this model may represent some aspects of the pathophysiology of NASH.

In contrast, candesartan cilexetil did not improve hepatic injury, steatosis and fibrosis in this model, unlike previous preclinical reports for ARBs. As this model did not have phenotypes leading to insulin resistance such as obesity and hyperglycemia,

the effect of candesartan cilexetil might be underestimated in this model.

Chapter 4

Combination effects of alogliptin and pioglitazone in a mouse model of NASH

4.1 Objectives

Drug repositioning is a process to discover a marketed drug for a different indication. The process is generally applied in expectation of reduced time, risk and cost in pharmaceutical research and development [131]. One approach for repositioning of drugs is to find their new indications based on common pathophysiological traits or molecular pathways to their original indications. Given the close link of MS such as type 2 diabetes to NASH [25], repositioning of anti-diabetic drugs theoretically seems reasonable in order to deliver drugs to patients with NASH in a shorter time.

NASH is a complex disease where multiple factors act in parallel and are associated with the development and progression of disease [57]. Therefore, simultaneous inhibition of multiple targets may be required to show clinical benefit in NASH. In fact, several preclinical and clinical results suggest potential utility of combination therapy of anti-diabetic agents on NASH, e.g. combination of insulin and metformin on hepatic steatosis in NAFLD patients [132]. In addition, GFT505 showed preferable effects in NASH patients based on its PPARα and PPARδ activities [133]. Given these results, combination therapy or combination of different mechanisms would be an attractive medical approach to patients with NASH.

DPP-4 inhibitors are well-known anti-diabetic drugs widely used in clinic. Therapeutic effects of DPP-4 inhibitors as well as pioglitazone have been evaluated also in NASH owing to the common pathophysiological traits of type 2 diabetes and NASH. Several studies suggested DPP-4 inhibitors improved NASH clinically [94–96] and preclinically [134–138]. Sitagliptin improved hepatic ballooning, NASH scores, and plasma aminotransferase levels in NASH patients with type 2 diabetes in an open-label,

single-arm observational pilot study [94]. Sitagliptin also improved hepatic steatosis in patients with type 2 diabetes in a prospective, single-center, open-label comparative study [94]. Alogliptin decreased NAFIC score (diagnosed by serum ferritin, fasting insulin, and type IV collagen 7S) in NAFLD patients with type 2 diabetes in a single arm, multi-center, non-randomized study [95]. Interestingly, the anti-steatotic and anti-fibrotic effects of sitagliptin seem to be independent of the glucose-lowering effects in mice fed MCD diet [136].

Benefits of the concomitant use of pioglitazone and DPP-4 inhibitors has been well-demonstrated in type 2 diabetes [139,140], and their fixed-dose combination products have been marketed. A single tablet by the fixed-dose combination should be considerable to achieve better compliance to therapy. Given their anti-fibrotic and anti-inflammatory potentials besides glucose-lowering effects [136,141–143], we hypothesized that combination therapy using pioglitazone and a DPP-4 inhibitor would provide additional clinical benefits in the treatment of NASH. Combination effects of pioglitazone and a DPP-4 inhibitor on NASH have never been evaluated either preclinically or clinically.

In case pioglitazone is thought to be one of drugs in a single tablet, metformin plus pioglitazone is another candidate of a fixed-dose combination [144] and may be potential combination therapy for NASH patients with type 2 diabetes. Although the fixed-dose combination has never been tried in NASH either preclinically or clinically, clinical evidence does not support therapeutic role of metformin monotherapy in NAFLD [145], and use of metformin in NASH patients is not recommended in the guideline [3].

Therefore, the purpose of this study was to evaluate a concomitant treatment of

pioglitazone and a DPP-4 inhibitor alogliptin against their monotherapies in a non-obese and normoglycemic animal model of NASH. To our knowledge, this is the first report to show combination utility of DPP-4 inhibitor and pioglitazone in NASH.

4.2 Materials and methods

4.2.1 Animals

All animal experiments were carried out according to the guidelines of the Institutional Animal Care and Use Committee in Takeda Pharmaceutical Company Ltd. $LDLR^{-/-}$ mice fed a modified CDAA diet were used as an animal model of NASH as described in Chapter 2. Breeding pairs of homozygous $LDLR^{-/-}$ mice were obtained from Jackson Laboratories, and a colony was maintained at Takeda Rabics. Six-week-old male $LDLR^{-/-}$ mice were used. The mice were acclimatized on a normal chow diet and subsequently fed either chow or a modified CDAA diet.

4.2.2 Drug administration

Alogliptin benzoate and pioglitazone hydrochloride were synthesized at Takeda Pharmaceutical Company Ltd. The doses of alogliptin and pioglitazone were expressed as the free base form. In a single-dosing study, alogliptin (30–200 mg/kg) was orally administered to the mice (n = 6). For the multiple-dose monotherapy, alogliptin (10–200 mg/kg) and pioglitazone (6–20 mg/kg) were orally administered to the mice once daily for 7 weeks; the administration commenced after the mice had received the modified

CDAA diet for 1 week (n = 10). For the multiple-dose combination therapy, alogliptin (30 mg/kg), pioglitazone (20 mg/kg), and their combination were orally administered for 3 weeks to the mice fed the diet for 1 week (n = 16). Mice in the control groups were given orally 0.5% methylcellulose solution once daily (5 mL/kg, n = 4–16).

4.2.3 Sample collection

Blood samples were collected from the tail vein under a non-fasted state. In the pharmacodynamic study, blood samples were collected over time after the single dosing. After the multiple-dosing studies, the mice were anesthetized under a non-fasted state and euthanized by over-bleeding from the abdominal aorta. Whole liver and adipose tissue weights were measured. Liver samples from the left lateral lobes were immediately separated and stored as formalin-fixed, frozen, or fixed in RNAlater (Life Technologies) for subsequent analyses.

4.2.4 Plasma DPP-4 assay

The plasma DPP-4 assay was carried out in accordance with a previous report [146]. In detail, 10 μL of the plasma sample was mixed with 90 μL of reagent (100 μmol/L H-Gly-Pro-7-amino-4-methylcoumarin; Bachem, Bubendorf, Switzerland) and incubated for 30 min. After incubation, the reaction was stopped with the addition of 100 μL of 25% acetic acid. For the reaction controls, 10 μL of the plasma samples was mixed with 100 μL of 25% acetic acid and 90 μL of the substrate. To generate a standard curve, H-Gly-Pro-7-amino-4-methylcoumarin was serially diluted 100 μL of

the H-Gly-Pro-7-amino-4-methylcoumarin solutions in each concentration were mixed with 100 μL of 25% acetic acid. The release of H-Gly-Pro-7-amino-4-methylcoumarin was measured fluorometrically at an excitation wavelength of 380 nm and an emission wavelength of 460 nm. The fluorescence intensity of each sample was calculated by the subtraction of the control fluorescent intensity from the sample fluorescent intensity. From the standard curve, H-Gly-Pro-7-amino-4-methylcoumarin content (μmol/L) was calculated by the fluorescence intensity. DPP-4 activity (nmol/min/mL) was calculated by the following formula: H-Gly-Pro-7-amino-4-methylcoumarin content (μmol/L) × reaction volume (0.1 mL)/sample volume (0.01 mL)/reaction time (30 min). The inhibition rate of DPP-4 activity was defined as the DPP-4 activity of each sample divided by the DPP-4 activity of the vehicle sample, and expressed as a percentage.

4.2.5 Blood biochemistry

Plasma glucose, non-esterified fatty acid, and ALT levels were measured using an automatic analyzer.

4.2.6 Histological evaluation

The quantitative analysis of Sirius red-positive fibrosis areas was performed as described in Chapter 2 and 3. In brief, livers were fixed in 10% neutral buffered formalin, embedded in paraffin, sectioned, and stained with Sirius red. Four bright field images of a stained section of the left lateral lobe for each animal were captured by using a BX53 microscope and a DP-20 digital camera. Fibrosis areas were evaluated

using the WinROOF image analyzing system and the results were determined as the mean of the four fields of each section.

4.2.7 Measurement of hepatic triglyceride levels

Hepatic triglyceride levels were measured as described in Chapter 2 and 3. Briefly, frozen liver samples were homogenized in Na_2SO_4 solution and the total lipids were extracted with hexane and 2-propanol. The levels of triglycerides in the lipid extract were measured using an automatic analyzer.

4.2.8 Measurement of liver mRNA levels

Hepatic gene expression was measured as described in Chapter 2 and 3. Total RNA was isolated from the liver samples that were stored in RNAlater. The gene expression was quantified using a *Taq*Man real-time polymerase chain reaction using the ABI prism 7900HT Sequence Detection system and normalized to the expression of glyceraldehyde 3-phosphate dehydrogenase.

4.2.9 Measurement of cytokine and chemokine levels in liver homogenates

The frozen liver samples were homogenized with RIPA buffer (Wako Pure Chemicals Ltd, Osaka, Japan) that contained protease inhibitor cocktail III (Wako Pure Chemicals Ltd). These homogenates were centrifuged and the supernatants were collected. The Bio-Plex analysis in the supernatants was carried out in accordance with

the manufacturer's instructions (Bio-Rad, Hercules, CA, U.S.A.). The protein concentration of the supernatant was determined by using a BCA Protein Assay Kit (Thermo Fisher Scientific, Waltham, MA, U.S.A.). The results from Bio-Plex analysis were normalized to the protein concentration.

4.2.10 Statistical analysis

Statistical analyses were carried out with two-tailed Williams' test or two-tailed Shirley–Williams' test for monotherapy studies. Student's *t*-test or Aspin–Welch test was used to compare the combination therapy with a monotherapy. Values of $P < 0.05$ were considered statistically significant. The data are represented as the mean ± SD.

4.3 Results

4.3.1 Effects of alogliptin on plasma DPP-4 activity in the NASH model

In order to measure target engagement of alogliptin in the NASH model, plasma DPP-4 activity was measured. One hour after a single administration of alogliptin at doses of 30, 100, and 200 mg/kg, plasma DDP-4 activities were completely suppressed (Figure 18A). At all doses, the suppression was sustained for 24 h.

4.3.2 Effects of alogliptin and pioglitazone monotherapy in the NASH model

Based on the single-dose pharmacodynamic study, 10, 30, 60, and 200 mg/kg of

alogliptin were selected as the doses for the multiple-dose study. As pioglitazone exhibits hypoglycemic effects at doses in the range from 4–15 mg/kg in type 2 diabetic mice when as a diet admixture [147,148], the gavage doses of 6, 10, and 20 mg/kg were selected for this study.

Alogliptin showed a statistically significant reduction of hepatic triglyceride levels only at the highest dose (Figure 18B). In contrast, alogliptin significantly suppressed the area of hepatic fibrosis, where submaximal effects were observed at 30 mg/kg (Figure 18C). Alogliptin also reduced the hepatic gene expression of collagen-1 (Figure 18D). Hepatic triglyceride content was significantly reduced by pioglitazone at all dose levels (Figure 18B), whereas pioglitazone significantly decreased the area of hepatic fibrosis and collagen-1 expression only at 20 mg/kg (Figure 18C, D). Representative images of liver sections stained with Sirius red in mice fed normal chow diet, modified CDAA diet, 30 mg/kg alogliptin, and 20 mg/kg pioglitazone groups are shown in Figure 19A–D.

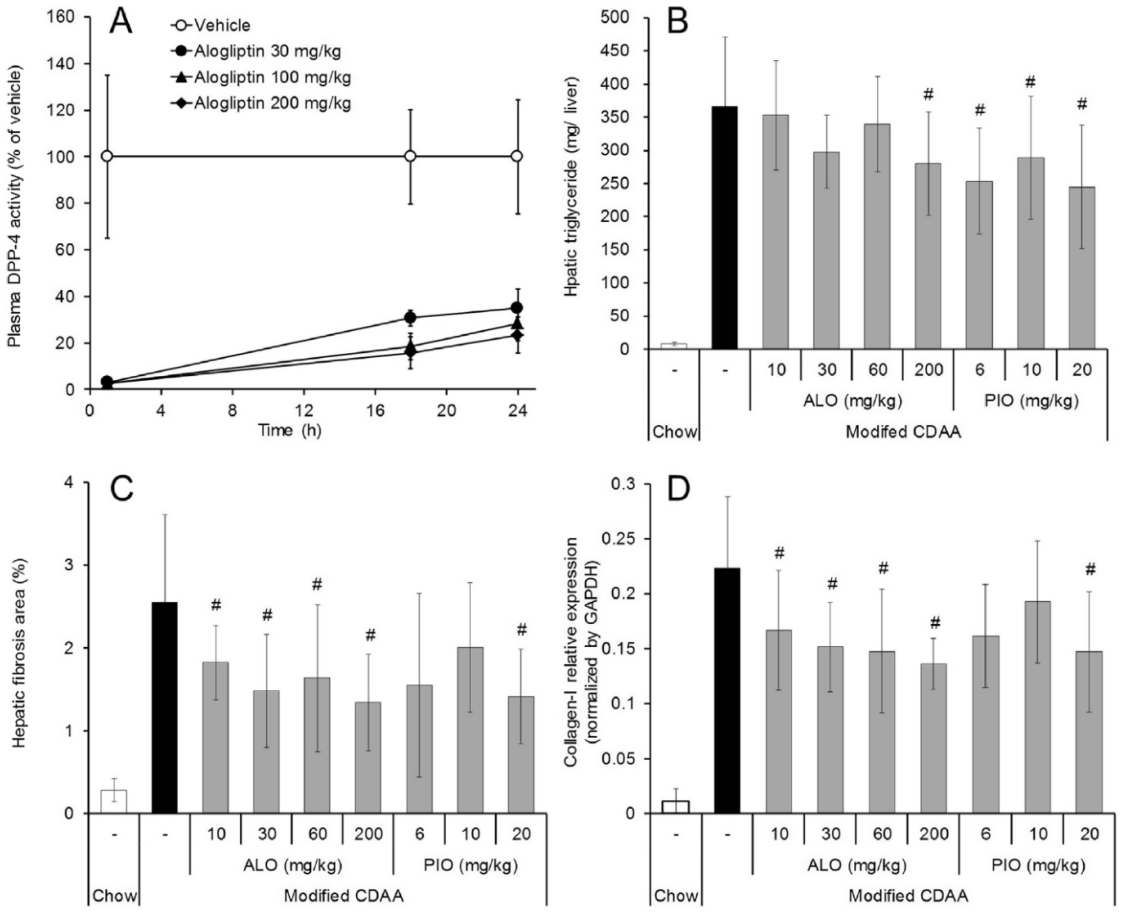

Figure 18 Effects of alogliptin and pioglitazone monotherapy on plasma DPP-4 activity, hepatic fibrosis area, gene expression of collagen-1, and hepatic triglyceride levels.

Plasma DPP-4 activities (A) were measured as described in Materials and methods (n = 6). Alogliptin (ALO; 10, 30, 60, and 200 mg/kg) and pioglitazone (PIO; 6, 10, and 20 mg/kg) were orally administered to the mice once daily for 7 weeks (n = 10). Hepatic triglyceride levels (B), hepatic fibrosis area (C), and hepatic gene expression of collagen-1 (D) were measured as described in Materials and methods. Gene expression was normalized by GAPDH expression. $^{\#}P < 0.05$ vs modified CDAA–control by two-tailed Williams' test. Mean ± SD.

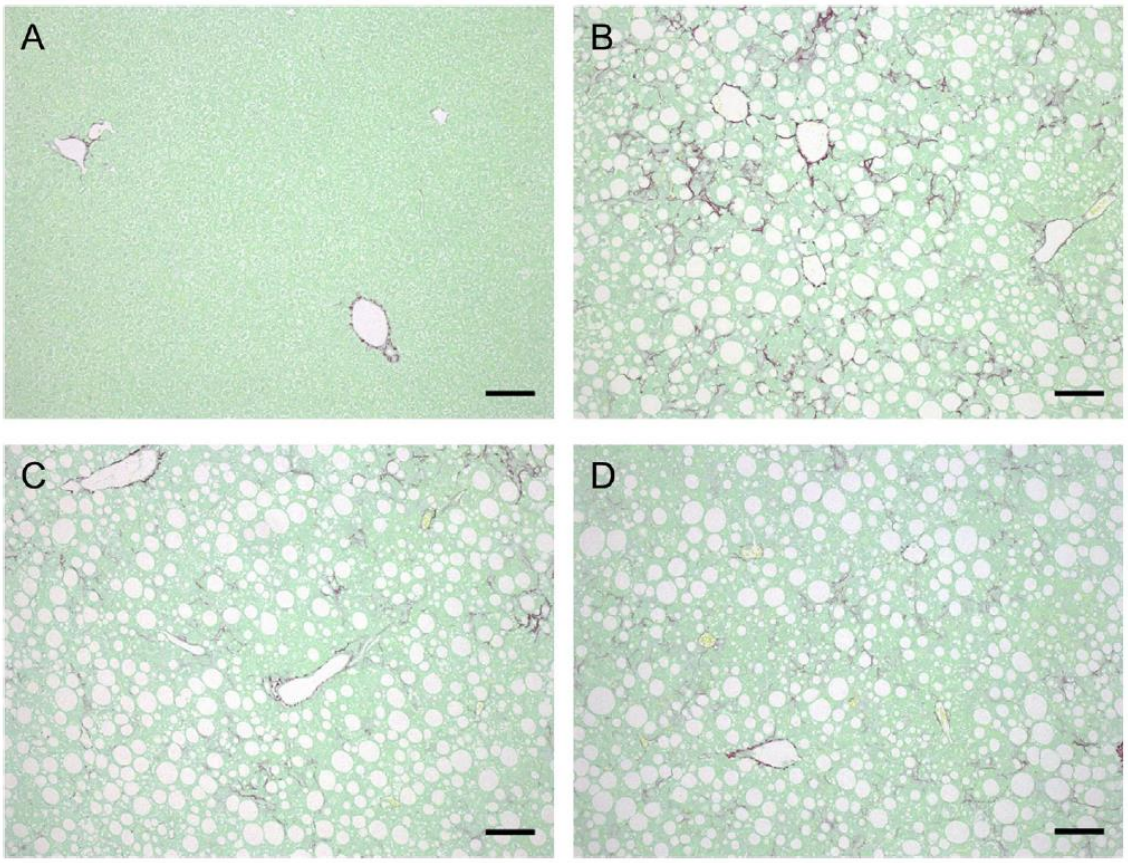

Figure 19　Representative images of liver sections stained with Sirius red.

Alogliptin and pioglitazone were orally administered to the mice once daily for 7 weeks. Representative images of liver sections from normal chow–control (A), modified CDAA–control (B), alogliptin 30 mg/kg-treated (C), and pioglitazone 20 mg/kg-treated groups (D) are shown. Scale bar = 100 μm.

4.3.3 Effects of combination therapy of alogliptin and pioglitazone in the NASH model

Compared with monotherapy, the concomitant treatment more potently reduced hepatic triglyceride levels (Figure 20A). The combination therapy also reduced collagen-1 gene expression, where the effect was significantly greater than that of monotherapy (Figure 20B).

The hepatic gene expression of CD11b, a marker of macrophage infiltration, was significantly decreased by pioglitazone, whereas alogliptin tended to decrease CD11b expression (Figure 20C). Several chemokines and cytokines such as MCP-1, macrophage inflammatory protein-1α, interferon-γ, interleukin-1α, and interleukin-12 in liver homogenate in mice fed the modified CDAA diet increased compared with those in the mice fed normal chow diet (data not shown). The combination therapy showed greater inhibition of MCP-1 than the alogliptin and pioglitazone monotherapy regimens (Figure 20D).

Body weight increased after the treatment with pioglitazone, whereas alogliptin treatment had no effect (Figure 21A). Neither monotherapy nor combination therapy affected plasma glucose level because the model did not show insulin resistance-derived hyperglycemia (Figure 21B). Plasma non-esterified fatty acid level was significantly reduced by pioglitazone, but the combination therapy showed a greater reduction (Figure 21C). Plasma ALT levels significantly decreased in all treatment groups (Figure 21D).

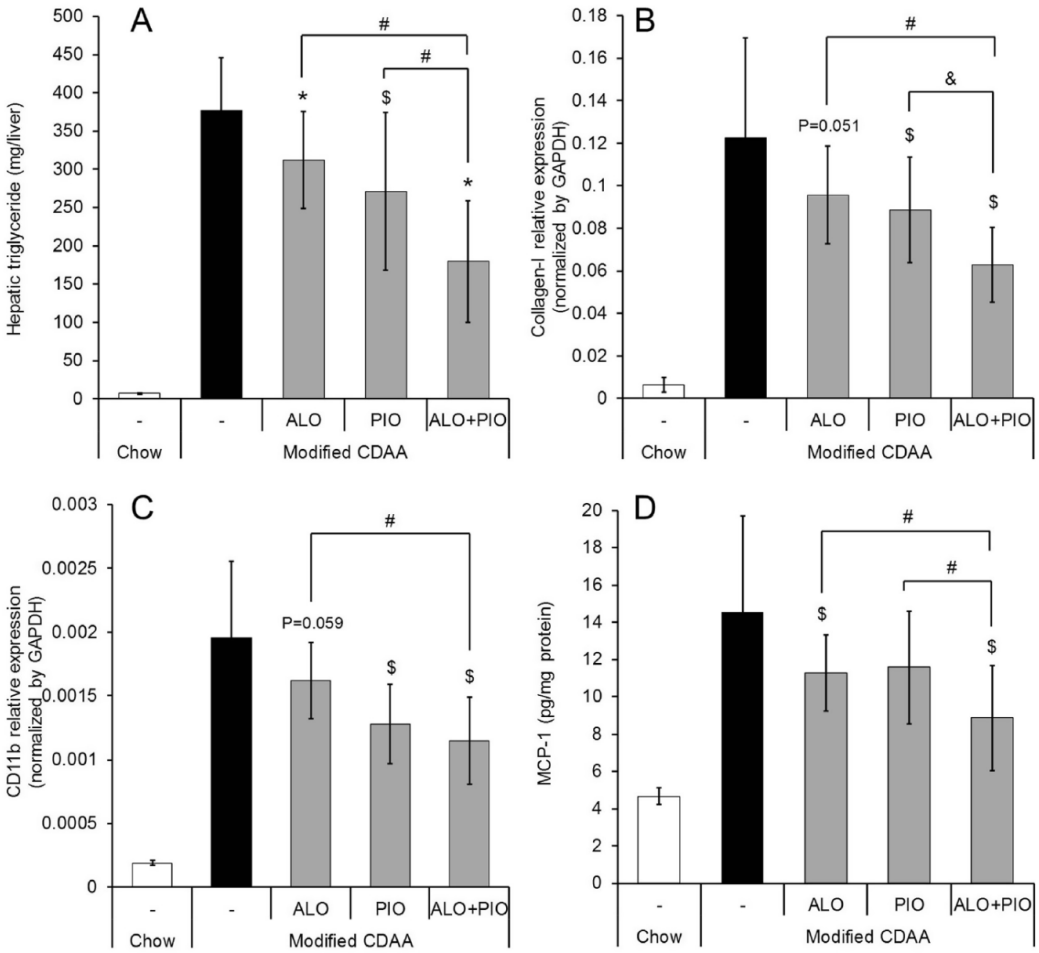

Figure 20 Effects of combination therapy on hepatic triglyceride levels, gene expression of collagen-1 and CD11b, and hepatic MCP-1 protein levels.

Alogliptin (ALO; 30 mg/kg), pioglitazone (PIO; 20 mg/kg), and their combination were orally administered to the mice once daily for 3 weeks (n = 16). Hepatic triglyceride levels (A), hepatic gene expression of collagen-1 (B) and CD11b (C), and MCP-1 levels in the liver homogenates (D) were measured as described in Materials and methods. Gene expression was normalized by GAPDH expression. $^{*}P < 0.05$ vs modified CDAA–control by Student's *t*-test, $^{\$}P < 0.05$ vs modified CDAA–control by Aspin–Welch test, $^{\#}P < 0.05$ vs monotherapy by Student's *t*-test, $^{\&}P < 0.05$ vs monotherapy by Aspin–Welch test. Mean ± SD.

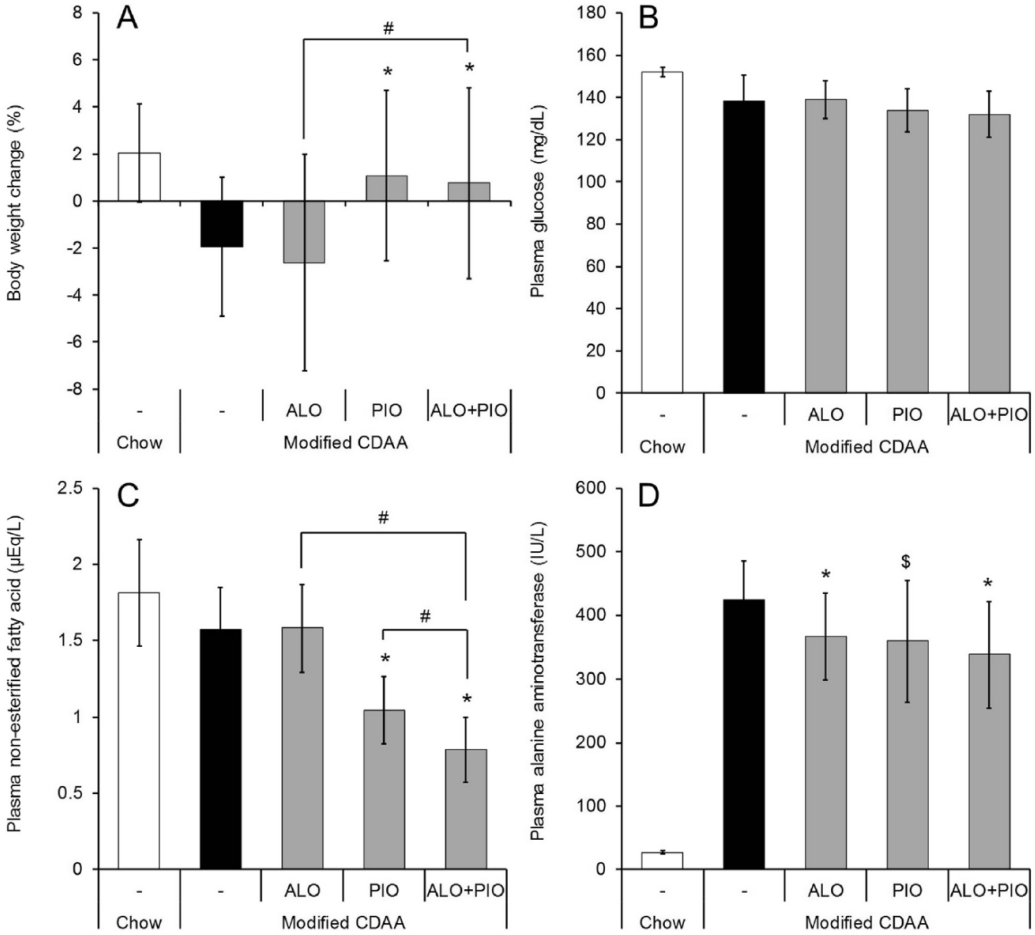

Figure 21 Effects of combination therapy on body weight gain and blood biochemistry.

Alogliptin (ALO; 30 mg/kg), pioglitazone (PIO; 20 mg/kg), and their combination were orally administered to the mice once daily for 3 weeks (n = 16). Body weight was monitored once per week throughout the treatment period, and body weight changes from the initial value were calculated (A). Plasma glucose (B), non-esterified fatty acid (C), and alanine aminotransferase levels (D) were measured using an automatic analyzer. *P < 0.05 vs modified CDAA–control by Student's t-test, $^{\$}P$ < 0.05 vs modified CDAA–control by Aspin–Welch test, $^{\#}P$ < 0.05 vs monotherapy by Student's t-test. Mean ± SD.

4.4 Discussion

The mechanistic relationship between DPP-4 inhibition and anti-fibrotic effects has not been fully elucidated, but in the current study, alogliptin resulted in significant improvement of both hepatic fibrosis and steatosis with sustained DPP-4 inhibition in a diet-induced NASH model with genetic dyslipidemic feature. Anti-steatotic effects of DPP-4 inhibitors independent from their glucose-lowering effects shown in elsewhere [134–136] were further confirmed as the NASH model we used was not hyperglycemic and the treatment with alogliptin had no effect on plasma glucose level. Underlying mechanisms of DPP-4 inhibition for anti-steatotic effect may include increased energy expenditure [134], decreased hepatic lipogenesis [137,138], and increased hepatic lipolysis [135] (Figure 22).

Extrahepatic mechanism such as adipose tissue-derived adiponectin is suggested to contribute to improvement of hepatic steatosis by pioglitazone under choline-deficient condition [149]. In the current study, as plasma fatty acid levels were significantly reduced by pioglitazone, similar extrahepatic mechanism such as inhibition of free fatty acid supplement from peripheral adipose tissue may contribute to the anti-steatotic effect of pioglitazone (Figure 22). As the mechanisms postulated for both alogliptin and pioglitazone on hepatic triglyceride reduction do not overlap and compensate each other, significant superiority of the combination therapy may be observed.

Chemokines play important roles in the pathophysiology of NASH [150]. During development of NASH, MCP-1 and its receptor were upregulated in the liver [151,152], where they promoted macrophage accumulation and inflammation [153]. Most recently Wang et al. [154] demonstrated inhibition of CD11b-positive inflammatory cell

infiltration and hepatic fibrosis formation with sitagliptin in a mouse model of NASH. DPP-4 can cleave N-terminal dipeptides of proline or alanine-containing peptides including incretin, neuropeptides and chemokines [155]. Furthermore, it was reported that MCP-1 contributed to the development of liver steatosis in $LDLR^{-/-}$ mice [156]. Accordingly, alogliptin-induced MCP-1 suppression observed in this study might be a mechanism underlying efficacy in this NASH model (Figure 22). Pioglitazone also reduced hepatic inflammatory area in mice fed a MCD diet [157]. In contrast, the targeted deletion of PPARγ in macrophages displayed an exacerbated response to higher necroinflammatory injury in the liver [158]. Collectively, the anti-chemotaxic properties of alogliptin and pioglitazone should result in the reduction of hepatic inflammatory marker CD11b in this model. The in vivo effects of alogliptin and pioglitazone on hepatic fibrosis, therefore, may be attributable to the inhibition of hepatic triglyceride accumulation and chemotaxic responses, at least in the NASH model used in this study (Figure 22).

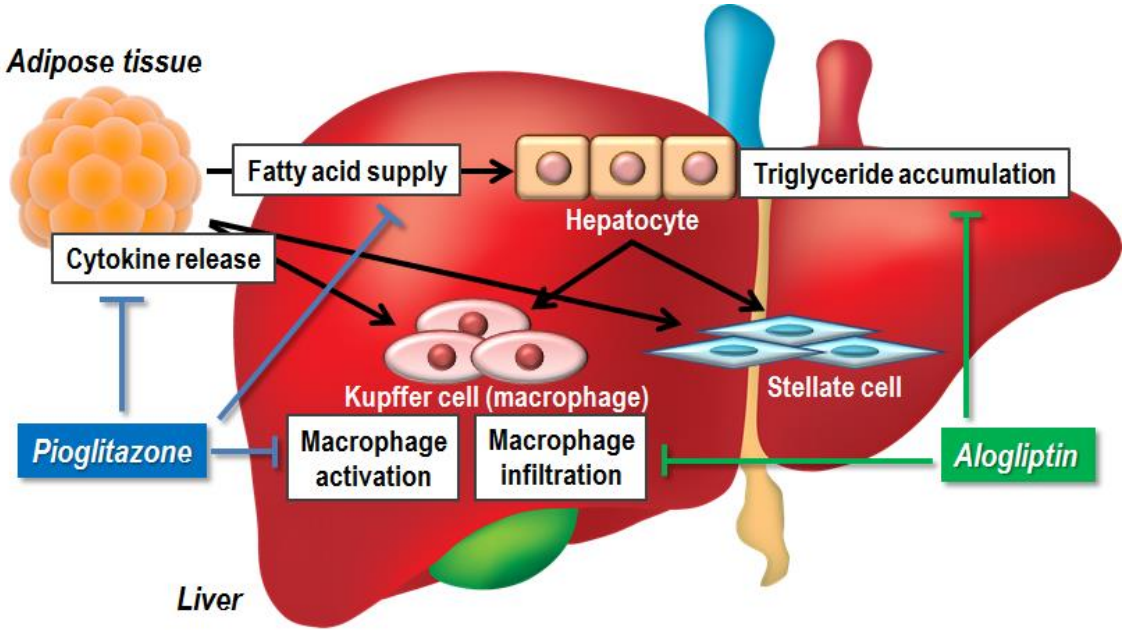

Figure 22 Postulated mechanism of actions of alogliptin and pioglitazone in nonalcoholic steatohepatitis.

4.5 Chapter summary

Monotherapy with alogliptin significantly improved hepatic fibrosis and steatosis with sustained plasma DPP-4 inhibition in $LDLR^{-/-}$ mice with modified CDAA. Alogliptin also decreased hepatic MCP-1, a chemokine related to macrophage accumulation.

Furthermore, the concomitant treatment of alogliptin and pioglitazone also decreased hepatic triglyceride and hepatic collagen-1 mRNA at a greater extent compared with their monotherapy. Hepatic expression of inflammatory markers including CD11b mRNA and MCP-1 were also reduced by the concomitant treatment. These results suggest that combination therapy using pioglitazone and a DPP-4 inhibitor may provide a novel therapeutic option for patients with type 2 diabetes and NASH.

Chapter 5

Conclusion

First of all, we established a mouse model which rapidly developed NASH-like phenotypes and advanced stages by combination of dietary challenge and genetic modification. Comprehensive profiling demonstrated that $LDLR^{-/-}$ mice with modified CDAA diet showed hepatic steatosis, inflammatory cell infiltration, hepatic injury, and hepatic fibrosis without showing obesity and diabetes (Chapter 2). Furthermore, this model showed advanced stages associated with NASH such as hepatocellular hyperplasia, adenoma, and carcinoma. The formation of hepatic fibrosis and hepatocellular carcinoma in this model tended to progress rapidly compared with other reported mouse models.

Next, the translatability of the model to NASH was further proven by a pharmacological approach using drugs with clinical evidence in NASH. Pioglitazone showed anti-fibrotic effects accompanied by improving hepatic transaminase activity and hepatic lipid accumulation in the model, which were similar to those reported in NASH patients (Chapter 3). On the other hand, some mechanisms, e.g. local renin-angiotensin system or insulin resistance would not always contribute to NASH formation in this animal model. Further profiling using other agents tested clinically will better clarify the utility of this model.

Finally, therapeutic effects of alogliptin, pioglitazone, and their combination were confirmed using the model (Chapter 4). Monotherapy with either alogliptin or pioglitazone significantly improved hepatic fibrosis and steatosis, which was not accompanied by glucose-lowering effect. Furthermore, the concomitant treatment of alogliptin and pioglitazone also decreased hepatic steatosis and fibrosis at a greater extent compared with their monotherapy.

In this research, we demonstrated the advantage by the combination therapy of

pioglitazone and alogliptin using a mouse model of NASH proven by pathophysiological and pharmacological approaches. These results suggest that a marketed fixed-dose combination of the two anti-diabetic drugs may be attractive therapeutic approach also for the treatment of NASH. The possibility should be explored in future controlled clinical trials.

Acknowledgements

本論文の作成にあたり、御懇篤なる御指導と御鞭撻を賜りました、徳島大学大学院　医歯薬学研究部　生命薬学系　生命薬理学分野　藤野裕道教授に深く感謝の意を表します。

本研究は終始、武田薬品工業株式会社　リサーチ　薬剤安全性研究所　アソシエイトサイエンティフィックフェロー　天野雄一郎氏およびアーサムセラピューティクス株式会社　長袋洋氏の親身な御指導のもと行われたものであり、ここに厚く御礼申し上げます。

また、本研究の遂行および本論文作成にあたり多くの御指導と御援助を頂きました武田薬品工業株式会社　リサーチ　再生医療ユニット　主席研究員　兎澤隆一氏、薬剤安全性研究所　主任研究員　安野弘修氏、薬物動態研究所　主任研究員　遠山季美夫氏、リサーチ　主席部員　松川純氏、日本開発センター　シニアクリニカルサイエンスダイレクター　河村栄美子氏、主席部員　塩谷和昭氏、アクセリードドラッグディスカバリーパートナーズ株式会社　研究本部　非臨床安全性研究　清水文氏、統合生物　原田絢子氏、武田コンシューマヘルスケア株式会社　製品開発部　課長代理　今井真由美氏、日本たばこ産業株式会社　磯野修氏、Cardurion Pharmaceuticals K.K. 淺田真理氏、株式会社スコヒアファーマ　安原吉高氏、及び今井重光氏に感謝致します。

最後に、本論文の作成は、家族の支えなくしては成し得なかったものであります。ここに深く感謝致します。

References

1. Vernon G, Baranova A, Younossi ZM. Systematic review: the epidemiology and natural history of non-alcoholic fatty liver disease and non-alcoholic steatohepatitis in adults. Aliment Pharmacol Ther. 2011;34(3):274–85.
2. Vanni E, Bugianesi E, Kotronen A, De Minicis S, Yki-Jarvinen H, Svegliati-Baroni G. From the metabolic syndrome to NAFLD or vice versa? Dig Liver Dis. 2010;42(5):320–30.
3. Chalasani N, Younossi Z, Lavine JE, Charlton M, Cusi K, Rinella M, Harrison SA, Brunt EM, Sanyal AJ. The diagnosis and management of nonalcoholic fatty liver disease: Practice guidance from the American Association for the Study of Liver Diseases. Hepatology. 2018;67(1):328–57.
4. Singh DK, Rastogi A, Sakhuja P, Gondal R, Sarin SK. Comparison of clinical, biochemical and histological features of alcoholic steatohepatitis and non-alcoholic steatohepatitis in Asian Indian patients. Indian J Pathol Microbiol. 2010;53(3):408–13.
5. Matteoni CA, Younossi ZM, Gramlich T, Boparai N, Liu YC, McCullough AJ. Nonalcoholic fatty liver disease: a spectrum of clinical and pathological severity. Gastroenterology. 1999 Jun;116(6):1413–9.
6. Kleiner DE, Brunt EM, Van Natta M, Behling C, Contos MJ, Cummings OW, Ferrell LD, Liu YC, Torbenson MS, Unalp-Arida A, Yeh M, McCullough AJ, Sanyal AJ, Nonalcoholic Steatohepatitis Clinical Research N. Design and validation of a histological scoring system for nonalcoholic fatty liver disease. Hepatology. 2005;41(6):1313–21.

7. Angulo P. GI epidemiology: nonalcoholic fatty liver disease. Aliment Pharmacol Ther. 2007 Apr 15;25(8):883–9.

8. Williams CD, Stengel J, Asike MI, Torres DM, Shaw J, Contreras M, Landt CL, Harrison SA. Prevalence of nonalcoholic fatty liver disease and nonalcoholic steatohepatitis among a largely middle-aged population utilizing ultrasound and liver biopsy: a prospective study. Gastroenterology. 2011;140(1):124–31.

9. Radu C, Grigorescu M, Crisan D, Lupsor M, Constantin D, Dina L. Prevalence and associated risk factors of non-alcoholic fatty liver disease in hospitalized patients. J Gastrointestin Liver Dis. 2008;17(3):255–60.

10. Bae JC, Cho YK, Lee WY, Seo H Il, Rhee EJ, Park SE, Park CY, Oh KW, Sung KC, Kim BI. Impact of nonalcoholic fatty liver disease on insulin resistance in relation to HbA1c levels in nondiabetic subjects. Am J Gastroenterol. 2010;105(11):2389–95.

11. Das K, Das K, Mukherjee PS, Ghosh A, Ghosh S, Mridha AR, Dhibar T, Bhattacharya B, Bhattacharya D, Manna B, Dhali GK, Santra A, Chowdhury A. Nonobese population in a developing country has a high prevalence of nonalcoholic fatty liver and significant liver disease. Hepatology. 2010;51(5):1593–602.

12. Hou X, Zhu Y, Lu H, Chen H, Li Q, Jiang S, Xiang K, Jia W. Non-alcoholic fatty liver disease's prevalence and impact on alanine aminotransferase associated with metabolic syndrome in the Chinese. J Gastroenterol Hepatol. 2011;26(4):722–30.

13. Chen Z, Chen L, Dai H, Chen J, Fang L. Relationship between alanine aminotransferase levels and metabolic syndrome in nonalcoholic fatty liver

disease. J Zhejiang Univ Sci B. 2008;9(8):616–22.

14. Eguchi Y, Hyogo H, Ono M, Mizuta T, Ono N, Fujimoto K, Chayama K, Saibara T, Jsg N. Prevalence and associated metabolic factors of nonalcoholic fatty liver disease in the general population from 2009 to 2010 in Japan: a multicenter large retrospective study. J Gastroenterol. 2012;47(5):586–95.
15. el-Hassan AY, Ibrahim EM, Al-Mulhim FA, Nabhan AA, Chammas MY. Fatty infiltration of the liver: analysis of prevalence, radiological and clinical features and influence on patient management. Br J Radiol. 1992 Sep;65(777):774–8.
16. Browning JD. Statins and hepatic steatosis: Perspectives from the Dallas heart study. Hepatology. 2006;44(2):466–71.
17. Diehl AM, Goodman Z, Ishak KG. Alcohollike liver disease in nonalcoholics. A clinical and histologic comparison with alcohol-induced liver injury. Gastroenterology. 1988;95(4):1056–62.
18. Lee RG. Nonalcoholic steatohepatitis: a study of 49 patients. Hum Pathol. 1989 Jun;20(6):594–8.
19. Ong JP, Younossi ZM. Epidemiology and natural history of NAFLD and NASH. Clin Liver Dis. 2007 Feb;11(1):1–16, vii.
20. Ferlay J, Soerjomataram I, Dikshit R, Eser S, Mathers C, Rebelo M, Parkin DM, Forman D, Bray F. Cancer incidence and mortality worldwide: Sources, methods and major patterns in GLOBOCAN 2012. Int J Cancer. 2015;136(5):E359–86.
21. Wong RJ, Cheung R, Ahmed A. Nonalcoholic steatohepatitis is the most rapidly growing indication for liver transplantation in patients with hepatocellular carcinoma in the U.S. Hepatology. 2014;59(6):2188–95.
22. Kohli A, Shaffer A, Sherman A, Kottilil S. Treatment of hepatitis C a systematic

review. JAMA - J Am Med Assoc. 2014;312(6):631–40.

23. Qiao Q, Gao W, Zhang L, Nyamdorj R, Tuomilehto J. Metabolic syndrome and cardiovascular disease. Ann Clin Biochem. 2007 May;44(Pt 3):232–63.

24. Dunstan DW, Zimmet PZ, Welborn TA, De Courten MP, Cameron AJ, Sicree RA, Dwyer T, Colagiuri S, Jolley D, Knuiman M, Atkins R, Shaw JE. The rising prevalence of diabetes and impaired glucose tolerance: the Australian Diabetes, Obesity and Lifestyle Study. Diabetes Care. 2002;25(5):829–34.

25. Bellentani S, Scaglioni F, Marino M, Bedogni G. Epidemiology of non-alcoholic fatty liver disease. Dig Dis. 2010 Jan;28(1):155–61.

26. Jimba S, Nakagami T, Takahashi M, Wakamatsu T, Hirota Y, Iwamoto Y, Wasada T. Prevalence of non-alcoholic fatty liver disease and its association with impaired glucose metabolism in Japanese adults. Diabet Med. 2005;22(9):1141–5.

27. Komeda T. Obesity and NASH in Japan. Hepatol Res. 2005 Oct;33(2):83–6.

28. Marchesini G, Bugianesi E, Forlani G, Cerrelli F, Lenzi M, Manini R, Natale S, Vanni E, Villanova N, Melchionda N, Rizzetto M. Nonalcoholic fatty liver, steatohepatitis, and the metabolic syndrome. Hepatology. 2003 Apr;37(4):917–23.

29. Adams LA, Lymp JF, St. Sauver J, Sanderson SO, Lindor KD, Feldstein A, Angulo P. The natural history of nonalcoholic fatty liver disease: A population-based cohort study. Gastroenterology. 2005;129(1):113–21.

30. Younossi ZM, Koenig AB, Abdelatif D, Fazel Y, Henry L, Wymer M. Global epidemiology of nonalcoholic fatty liver disease—Meta-analytic assessment of prevalence, incidence, and outcomes. Hepatology. 2016;64(1):73–84.

31. Angulo P, Kleiner D, Dam-Larsen S, Adams LA, Bjornsson ES, Charatcharoenwitthaya P, Mills PR, Keach JC, Lafferty HD, Stahler A, Haflidadottir S, Bendsten F. Liver Fibrosis, but no Other Histologic Features, Associates with Long-term Outcomes of Patients With Nonalcoholic Fatty Liver Disease. Gastroenterology. 2015;149(2):389–97.

32. Day CP, James OF. Steatohepatitis: a tale of two "hits"? Gastroenterology. 1998 Apr;114(4):842–5.

33. Fabbrini E, Mohammed BS, Magkos F, Korenblat KM, Patterson BW, Klein S. Alterations in adipose tissue and hepatic lipid kinetics in obese men and women with nonalcoholic fatty liver disease. Gastroenterology. 2008 Feb;134(2):424–31.

34. Postic C, Girard J. Contribution of de novo fatty acid synthesis to hepatic steatosis and insulin resistance: Lessons from genetically engineered mice. J Clin Invest. 2008;118(3):829–38.

35. Chitturi S, Abeygunasekera S, Farrell GC, Holmes-Walker J, Hui JM, Fung C, Karim R, Lin R, Samarasinghe D, Liddle C, Weltman M, George J. NASH and insulin resistance: Insulin hypersecretion and specific association with the insulin resistance syndrome. Hepatology. 2002 Feb;35(2):373–9.

36. Chalasani N, Deeg MA, Persohn S, Crabb DW. Metabolic and anthropometric evaluation of insulin resistance in nondiabetic patients with nonalcoholic steatohepatitis. Am J Gastroenterol. 2003;98(8):1849–55.

37. Marchesini G, Brizi M, Morselli-Labate AM, Bianchi G, Bugianesi E, McCullough AJ, Forlani G, Melchionda N. Association of nonalcoholic fatty liver disease with insulin resistance. Am J Med. 1999;107(5):450–5.

38. Donnelly KL, Smith CI, Schwarzenberg SJ, Jessurun J, Boldt MD, Parks EJ.

Sources of fatty acids stored in liver and secreted via lipoproteins in patients with nonalcoholic fatty liver disease. J Clin Invest. 2005;115(5):1343–51.

39. Diraison F, Moulin P, Beylot M. Contribution of hepatic de novo lipogenesis and reesterification of plasma non esterified fatty acids to plasma triglyceride synthesis during non-alcoholic fatty liver disease. Diabetes Metab. 2003 Nov;29(5):478–85.

40. Miele L, Grieco A, Armuzzi A, Candelli M, Forgione A, Gasbarrini A, Gasbarrini G. Hepatic mitochondrial beta-oxidation in patients with nonalcoholic steatohepatitis assessed by 13 C-octanoate breath test. Am J Gastroenterol. 2003;98(10):2335–6.

41. Fabbrini E, Magkos F, Mohammed BS, Pietka T, Abumrad NA, Patterson BW, Okunade A, Klein S. Intrahepatic fat, not visceral fat, is linked with metabolic complications of obesity. Proc Natl Acad Sci. 2009;106(36):15430–5.

42. Grattagliano I, Caraceni P, Portincasa P, Domenicali M, Palmieri VO, Trevisani F, Bernardi M, Palasciano G. Adaptation of subcellular glutathione detoxification system to stress conditions in choline-deficient diet induced rat fatty liver. Cell Biol Toxicol. 2003 Nov;19(6):355–66.

43. Leroux A, Ferrere G, Godie V, Cailleux F, Renoud ML, Gaudin F, Naveau S, Prévot S, Makhzami S, Perlemuter G, Cassard-Doulcier AM. Toxic lipids stored by Kupffer cells correlates with their pro-inflammatory phenotype at an early stage of steatohepatitis. J Hepatol. 2012;57(1):141–9.

44. Walenbergh SMA, Koek GH, Bieghs V, Shiri-Sverdlov R. Non-alcoholic steatohepatitis: The role of oxidized low-density lipoproteins. J Hepatol. 2013;58(4):801–10.

45. Canbay A, Feldstein AE, Higuchi H, Werneburg N, Grambihler A, Bronk SF, Gores GJ. Kupffer Cell Engulfment of Apoptotic Bodies Stimulates Death Ligand and Cytokine Expression. Hepatology. 2003;38(5):1188–98.

46. Chawla A, Nguyen KD, Goh YPS. Macrophage-mediated inflammation in metabolic disease. Nat Rev Immunol. 2011 Oct 10;11(11):738–49.

47. Negrin KA, Flach RJR, DiStefano MT, Matevossian A, Friedline RH, Jung D, Kim JK, Czech MP. IL-1 Signaling in obesity-induced hepatic lipogenesis and steatosis. PLoS One. 2014;9(9).

48. Tosello-Trampont AC, Landes SG, Nguyen V, Novobrantseva TI, Hahn YS. Kuppfer cells trigger nonalcoholic steatohepatitis development in diet-induced mouse model through tumor necrosis factor-α production. J Biol Chem. 2012;287(48):40161–72.

49. Gadd VL, Skoien R, Powell EE, Fagan KJ, Winterford C, Horsfall L, Irvine K, Clouston AD. The portal inflammatory infiltrate and ductular reaction in human nonalcoholic fatty liver disease. Hepatology. 2014;59(4):1393–405.

50. Rensen SS, Bieghs V, Xanthoulea S, Arfianti E, Bakker JA, Shiri-Sverdlov R, Hofker MH, Greve JW, Buurman WA. Neutrophil-derived myeloperoxidase aggravates non-alcoholic steatohepatitis in low-density lipoprotein receptor-deficient mice. PLoS One. 2012;7(12):e52411.

51. Rensen SS, Slaats Y, Nijhuis J, Jans A, Bieghs V, Driessen A, Malle E, Greve JW, Buurman WA. Increased hepatic myeloperoxidase activity in obese subjects with nonalcoholic steatohepatitis. Am J Pathol. 2009;175(4):1473–82.

52. Pulli B, Ali M, Iwamoto Y, Zeller MWG, Schob S, Linnoila JJ, Chen JW. Myeloperoxidase–Hepatocyte–Stellate Cell Cross Talk Promotes Hepatocyte

Injury and Fibrosis in Experimental Nonalcoholic Steatohepatitis. Antioxid Redox Signal. 2015;23(16):1255–69.

53. Chatzigeorgiou A, Karalis KP, Bornstein SR, Chavakis T. Lymphocytes in obesity-related adipose tissue inflammation. Diabetologia. 2012;55(10):2583–92.

54. Arita Y, Kihara S, Ouchi N, Takahashi M, Maeda K, Miyagawa JI, Hotta K, Shimomura I, Nakamura T, Miyaoka K, Kuriyama H, Nishida M, Yamashita S, Okubo K, Matsubara K, Muraguchi M, Ohmoto Y, Funahashi T, Matsuzawa Y. Paradoxical decrease of an adipose-specific protein, adiponectin, in obesity. Biochem Biophys Res Commun. 1999;257(1):79–83.

55. Friedman SL. Hepatic stellate cells: protean, multifunctional, and enigmatic cells of the liver. Physiol Rev. 2008 Jan;88(1):125–72.

56. Dooley S, Ten Dijke P. TGF-β in progression of liver disease. Cell Tissue Res. 2012;347(1):245–56.

57. Buzzetti E, Pinzani M, Tsochatzis EA. The multiple-hit pathogenesis of non-alcoholic fatty liver disease (NAFLD). Metabolism. 2016;65(8):1038–48.

58. Wands JR, Fava J, Wing RR. Randomized Controlled Trial Testing the Effects of Weight Loss on Nonalcoholic Steatohepatitis (NASH). 2011;51(1):121–9.

59. Musso G, Gambino R, Cassader M. Non-alcoholic fatty liver disease from pathogenesis to management: An update. Obes Rev. 2010;11(6):430–45.

60. Sanyal AJ, Chalasani N, Kowdley K V., McCullough A, Diehl AM, Bass NM, Neuschwander-Tetri BA, Lavine JE, Tonascia J, Unalp A, Van Natta M, Clark J, Brunt EM, Kleiner DE, Hoofnagle JH, Robuck PR. Pioglitazone, Vitamin E, or Placebo for Nonalcoholic Steatohepatitis. N Engl J Med. 2010;362(18):1675–85.

61. Klein E a, Jr IMT, Tangen CM, John J, Lucia MS, Goodman PJ, Minasian L,

Ford G, Parnes HL, Gaziano JM, Karp DD, Lieber MM, Walther PJ, Klotz L. Vitamin E and the Risk of Prostate Cancer: Updated Results of The Selenium and Vitamin E Cancer Prevention Trial (SELECT). J Am Med Assoc. 2011;306(14):1549–56.

62. Miller ER, Pastor-Barriuso R, Dalal D, Riemersma RA, Appel LJ, Guallar E. Meta-analysis: high-dosage vitamin E supplementation may increase all-cause mortality. Ann Intern Med. 2005 Jan 4;142(1):37–46.

63. Boettcher E, Csako G, Pucino F, Wesley R, Loomba R. Meta-analysis: pioglitazone improves liver histology and fibrosis in patients with non-alcoholic steatohepatitis. Aliment Pharmacol Ther. 2012;35(1):66–75.

64. Yau H, Rivera K, Lomonaco R, Cusi K. The future of thiazolidinedione therapy in the management of type 2 diabetes mellitus. Curr Diab Rep. 2013;13(3):329–41.

65. Schwenger KJ, Allard JP. Clinical approaches to non-alcoholic fatty liver disease. World J Gastroenterol. 2014;20(7):1712–23.

66. Cassidy S, Syed BA. Nonalcoholic steatohepatitis (NASH) drugs market. Nat Rev Drug Discov. 2016 Nov 3;15(11):745–6.

67. Neuschwander-Tetri BA, Loomba R, Sanyal AJ, Lavine JE, Van Natta ML, Abdelmalek MF, Chalasani N, Dasarathy S, Diehl AM, Hameed B, Kowdley K V, McCullough A, Terrault N, Clark JM, Tonascia J, Brunt EM, Kleiner DE, Doo E, NASH Clinical Research Network. Farnesoid X nuclear receptor ligand obeticholic acid for non-cirrhotic, non-alcoholic steatohepatitis (FLINT): a multicentre, randomised, placebo-controlled trial. Lancet (London, England). 2015 Mar 14;385(9972):956–65.

68. Staels B, Rubenstrunk A, Noel B, Rigou G, Delataille P, Millatt LJ, Baron M, Lucas A, Tailleux A, Hum DW, Ratziu V, Cariou B, Hanf R. Hepatoprotective effects of the dual peroxisome proliferator-activated receptor alpha/delta agonist, GFT505, in rodent models of nonalcoholic fatty liver disease/nonalcoholic steatohepatitis. Hepatology. 2013;58(6):1941–52.

69. Ratziu V, Harrison SA, Francque S, Bedossa P, Lehert P, Serfaty L, Romero-Gomez M, Boursier J, Abdelmalek M, Caldwell S, Drenth J, Anstee QM, Hum D, Hanf R, Roudot A, Megnien S, Staels B, Sanyal A, Mathurin P, Gournay J, Nguyen-Khac E, De Ledinghen V, Larrey D, Tran A, Bourliere M, Maynard-Muet M, Asselah T, Henrion J, Nevens F, Cassiman D, Geerts A, Moreno C, Beuers UH, Galle PR, Spengler U, Bugianesi E, Craxi A, Angelico M, Fargion S, Voiculescu M, Gheorghe L, Preotescu L, Caballeria J, Andrade RJ, Crespo J, Callera JL, Ala A, Aithal G, Abouda G, Luketic V, Huang MA, Gordon S, Pockros P, Poordad F, Shores N, Moehlen MW, Bambha K, Clark V, Satapathy S, Parekh S, Reddy RK, Sheikh MY, Szabo G, Vierling J, Foster T, Umpierrez G, Chang C, Box T, Gallegos-Orozco J. Elafibranor, an Agonist of the Peroxisome Proliferator-Activated Receptor-α and -δ, Induces Resolution of Nonalcoholic Steatohepatitis Without Fibrosis Worsening. Gastroenterology. 2016;150(5):1147–1159e5.

70. Haczeyni F, Yeh MM, Ioannou GN, Leclercq IA, Goldin R, Dan YY, Yu J, Teoh NC, Farrell GC. Mouse models of non-alcoholic steatohepatitis: A reflection on recent literature. J Gastroenterol Hepatol. 2018;33:1312–20.

71. Varela-Rey M, Embade N, Ariz U, Lu SC, Mato JM, Martinez-Chantar ML. Non-alcoholic steatohepatitis and animal models: understanding the human

disease. Int J Biochem Cell Biol. 2009;41(5):969–76.

72. Fan JG, Qiao L. Commonly used animal models of non-alcoholic steatohepatitis. Hepatobiliary Pancreat Dis Int. 2009;8(3):233–40.

73. Nakano S, Nagasawa T, Ijiro T, Inada Y, Tamura T, Maruyama K, Kuroda J, Yamazaki Y, Kusama H, Shibata N. Bezafibrate prevents hepatic stellate cell activation and fibrogenesis in a murine steatohepatitis model, and suppresses fibrogenic response induced by transforming growth factor-beta1 in a cultured stellate cell line. Hepatol Res. 2008 Oct;38(10):1026–39.

74. Yao ZM, Vance DE. Reduction in VLDL, but not HDL, in plasma of rats deficient in choline. Biochem Cell Biol. 1990 Feb;68(2):552–8.

75. Itagaki H, Shimizu K, Morikawa S, Ogawa K, Ezaki T. Morphological and functional characterization of non-alcoholic fatty liver disease induced by a methionine-choline-deficient diet in C57BL/6 mice. Int J Clin Exp Pathol. 2013;6(12):2683–96.

76. Takahashi Y, Soejima Y, Fukusato T. Animal models of nonalcoholic fatty liver disease/nonalcoholic steatohepatitis. World J Gastroenterol. 2012 May 21;18(19):2300–8.

77. Denda A, Kitayama W, Kishida H, Murata N, Tsutsumi M, Tsujiuchi T, Nakae D, Konishi Y. Development of hepatocellular adenomas and carcinomas associated with fibrosis in C57BL/6J male mice given a choline-deficient, L-amino acid-defined diet. Jpn J Cancer Res. 2002;93(2):125–32.

78. Matsumoto M, Hada N, Sakamaki Y, Uno A, Shiga T, Tanaka C, Ito T, Katsume A, Sudoh M. An improved mouse model that rapidly develops fibrosis in non-alcoholic steatohepatitis. Int J Exp Pathol. 2013 Apr 11;94(2):93–103.

79. Ikuta T, Kanno K, Arihiro K, Matsuda S, Kishikawa N, Fujita K, Tazuma S. Spontaneously hypertensive rats develop pronounced hepatic steatosis induced by choline-deficient diet: Evidence for hypertension as a potential enhancer in non-alcoholic steatohepatitis. Hepatol Res. 2012;42(3):310–20.

80. Bieghs V, Van Gorp PJ, Wouters K, Hendrikx T, Gijbels MJ, van Bilsen M, Bakker J, Binder CJ, Lütjohann D, Staels B, Hofker MH, Shiri-Sverdlov R. LDL receptor knock-out mice are a physiological model particularly vulnerable to study the onset of inflammation in non-alcoholic fatty liver disease. PLoS One. 2012 Jan;7(1):e30668.

81. Clapper JR, Hendricks MD, Gu G, Wittmer C, Dolman CS, Herich J, Athanacio J, Villescaz C, Ghosh SS, Heilig JS, Lowe C, Roth JD. Diet-induced mouse model of fatty liver disease and nonalcoholic steatohepatitis reflecting clinical disease progression and methods of assessment. Am J Physiol Gastrointest Liver Physiol. 2013;305(7):G483-95.

82. Dowman JK, Hopkins LJ, Reynolds GM, Nikolaou N, Armstrong MJ, Shaw JC, Houlihan DD, Lalor PF, Tomlinson JW, Hubscher SG, Newsome PN. Development of hepatocellular carcinoma in a murine model of nonalcoholic steatohepatitis induced by use of a high-fat/fructose diet and sedentary lifestyle. Am J Pathol. 2014;184(5):1550–61.

83. Subramanian S, Goodspeed L, Wang S, Kim J, Zeng L, Ioannou GN, Haigh WG, Yeh MM, Kowdley K V, O'Brien KD, Pennathur S, Chait A. Dietary cholesterol exacerbates hepatic steatosis and inflammation in obese LDL receptor-deficient mice. J Lipid Res. 2011;52(9):1626–35.

84. Tetri LH, Basaranoglu M, Brunt EM, Yerian LM, Neuschwander-Tetri BA.

Severe NAFLD with hepatic necroinflammatory changes in mice fed trans fats and a high-fructose corn syrup equivalent. Am J Physiol Gastrointest Liver Physiol. 2008;295(5):G987-95.

85. Ishibashi S, Brown MS, Goldstein JL, Gerard RD, Hammer RE, Herz J. Hypercholesterolemia in low density lipoprotein receptor knockout mice and its reversal by adenovirus-mediated gene delivery. J Clin Invest. 1993;92(2):883–93.

86. Ishibashi S, Goldstein JL, Brown MS, Herz J, Burns DK. Massive xanthomatosis and atherosclerosis in cholesterol-fed low density lipoprotein receptor-negative mice. J Clin Invest. 1994;93(5):1885–93.

87. Depner CM, Philbrick KA, Jump DB. Docosahexaenoic acid attenuates hepatic inflammation, oxidative stress, and fibrosis without decreasing hepatosteatosis in a Ldlr(-/-) mouse model of western diet-induced nonalcoholic steatohepatitis. J Nutr. 2013;143(3):315–23.

88. Gupte AA, Liu JZ, Ren Y, Minze LJ, Wiles JR, Collins AR, Lyon CJ, Pratico D, Finegold MJ, Wong ST, Webb P, Baxter JD, Moore DD, Hsueh WA. Rosiglitazone attenuates age- and diet-associated nonalcoholic steatohepatitis in male low-density lipoprotein receptor knockout mice. Hepatology. 2010;52(6):2001–11.

89. Wouters K, van Gorp PJ, Bieghs V, Gijbels MJ, Duimel H, Lütjohann D, Kerksiek A, van Kruchten R, Maeda N, Staels B, van Bilsen M, Shiri-Sverdlov R, Hofker MH. Dietary cholesterol, rather than liver steatosis, leads to hepatic inflammation in hyperlipidemic mouse models of nonalcoholic steatohepatitis. Hepatology. 2008 Aug;48(2):474–86.

90. Sahai A, Malladi P, Pan X, Paul R, Melin-Aldana H, Green RM, Whitington PF.

Obese and diabetic db/db mice develop marked liver fibrosis in a model of nonalcoholic steatohepatitis: role of short-form leptin receptors and osteopontin. Am J Physiol Gastrointest Liver Physiol. 2004;287(5):G1035-43.

91. Arsov T, Larter CZ, Nolan CJ, Petrovsky N, Goodnow CC, Teoh NC, Yeh MM, Farrell GC. Adaptive failure to high-fat diet characterizes steatohepatitis in Alms1 mutant mice. Biochem Biophys Res Commun. 2006;342(4):1152–9.

92. Kashireddy P V, Rao MS. Lack of peroxisome proliferator-activated receptor alpha in mice enhances methionine and choline deficient diet-induced steatohepatitis. Hepatol Res. 2004 Oct;30(2):104–10.

93. Carmiel-Haggai M, Cederbaum AI, Nieto N. A high-fat diet leads to the progression of non-alcoholic fatty liver disease in obese rats. FASEB J. 2005;19(1):136–8.

94. Yilmaz Y, Yonal O, Deyneli O, Celikel CA, Kalayci C, Duman DG. Effects of sitagliptin in diabetic patients with nonalcoholic steatohepatitis. Acta Gastroenterol Belg. 2012;75(2):240–4.

95. Mashitani T, Noguchi R, Okura Y, Namisaki T, Mitoro A, Ishii H, Nakatani T, Kikuchi E, Moriyasu H, Matsumoto M, Sato S, An T, Morita H, Aizawa S, Tokuoka Y, Ishikawa M, Matsumura Y, Ohira H, Kogure A, Noguchi K, Yoshiji H. Efficacy of alogliptin in preventing non-alcoholic fatty liver disease progression in patients with type 2 diabetes. Biomed Rep. 2016;4(2):183–7.

96. Kato H, Nagai Y, Ohta A, Tenjin A, Nakamura Y, Tsukiyama H, Sasaki Y, Fukuda H, Ohshige T, Terashima Y, Sada Y, Kondo A, Sasaoka T, Tanaka Y. Effect of sitagliptin on intrahepatic lipid content and body fat in patients with type 2 diabetes. Diabetes Res Clin Pr. 2015;109(1):199–205.

97. Feng R-N, Du S-S, Wang C, Li Y-C, Liu L-Y, Guo F-C, Sun C-H. Lean-non-alcoholic fatty liver disease increases risk for metabolic disorders in a normal weight Chinese population. World J Gastroenterol. 2014;20(47):17932–40.

98. Liu C-J. Prevalence and risk factors for non-alcoholic fatty liver disease in Asian people who are not obese. J Gastroenterol Hepatol. 2012;27(10):1555–60.

99. Thoolen B, Maronpot RR, Harada T, Nyska A, Rousseaux C, Nolte T, Malarkey DE, Kaufmann W, Kuttler K, Deschl U, Nakae D, Gregson R, Vinlove MP, Brix AE, Singh B, Belpoggi F, Ward JM. Proliferative and nonproliferative lesions of the rat and mouse hepatobiliary system. Toxicol Pathol. 2010;38(7 Suppl):5S–81S.

100. Caldwell S, Ikura Y, Dias D, Isomoto K, Yabu A, Moskaluk C, Pramoonjago P, Simmons W, Scruggs H, Rosenbaum N, Wilkinson T, Toms P, Argo CK, Al-Osaimi AM, Redick JA. Hepatocellular ballooning in NASH. J Hepatol. 2010;53(4):719–23.

101. Mormone E, George J, Nieto N. Molecular pathogenesis of hepatic fibrosis and current therapeutic approaches. Chem Biol Interact. 2011 Sep 30;193(3):225–31.

102. Ibusuki R, Uto H, Arima S, Mawatari S, Setoguchi Y, Iwashita Y, Hashimoto S, Maeda T, Tanoue S, Kanmura S, Oketani M, Ido A, Tsubouchi H. Transgenic expression of human neutrophil peptide-1 enhances hepatic fibrosis in mice fed a choline-deficient, L-amino acid-defined diet. Liver Int. 2013;33(10):1549–56.

103. Larter CZ, Yeh MM. Animal models of NASH: Getting both pathology and metabolic context right. J Gastroenterol Hepatol. 2008;23(11):1635–48.

104. Adkins Y, Schie IW, Fedor D, Reddy A, Nguyen S, Zhou P, Kelley DS, Wu J. A

novel mouse model of nonalcoholic steatohepatitis with significant insulin resistance. Lab Investig. 2013;93(12):1313–22.

105. Shiri-Sverdlov R, Wouters K, Gorp PJV, Gijbels MJ, Noel B, Buffat L, Staels B, Maeda N, Bilsen M Van, Hofker MH. Early diet-induced non-alcoholic steatohepatitis in APOE2 knock-in mice and its prevention by fibrates. J Hepatol. 2006;44(4):732–41.

106. Musso G, Gambino R, Cassader M. Cholesterol metabolism and the pathogenesis of non-alcoholic steatohepatitis. Prog Lipid Res. 2013;52(1):175–91.

107. Reynolds CM, McGillicuddy FC, Harford KA, Finucane OM, Mills KH, Roche HM. Dietary saturated fatty acids prime the NLRP3 inflammasome via TLR4 in dendritic cells-implications for diet-induced insulin resistance. Mol Nutr Food Res. 2012;56(8):1212–22.

108. Pfaffenbach KT, Gentile CL, Nivala AM, Wang D, Wei Y, Pagliassotti MJ. Linking endoplasmic reticulum stress to cell death in hepatocytes: roles of C/EBP homologous protein and chemical chaperones in palmitate-mediated cell death. Am J Physiol Endocrinol Metab. 2010 May;298(5):E1027-35.

109. Mells JE, Fu PP, Kumar P, Smith T, Karpen SJ, Anania FA. Saturated fat and cholesterol are critical to inducing murine metabolic syndrome with robust nonalcoholic steatohepatitis. J Nutr Biochem. 2015;26(3):285–92.

110. Sumiyoshi M, Sakanaka M, Kimura Y. Chronic intake of a high-cholesterol diet resulted in hepatic steatosis, focal nodular hyperplasia and fibrosis in non-obese mice. Br J Nutr. 2010;103(3):378–85.

111. Nie QH, Duan GR, Luo XD, Xie YM, Luo H, Zhou YX, Pan BR. Expression of TIMP-1 and TIMP-2 in rats with hepatic fibrosis. World J Gastroenterol.

2004;10(1):86–90.

112. Syn W-K, Choi SS, Liaskou E, Karaca GF, Agboola KM, Oo YH, Mi Z, Pereira T a, Zdanowicz M, Malladi P, Chen Y, Moylan C, Jung Y, Bhattacharya SD, Teaberry V, Omenetti A, Abdelmalek MF, Guy CD, Adams DH, Kuo PC, Michelotti G a, Whitington PF, Diehl AM. Osteopontin is induced by hedgehog pathway activation and promotes fibrosis progression in nonalcoholic steatohepatitis. Hepatology. 2011 Jan;53(1):106–15.

113. Sahai A, Malladi P, Melin-Aldana H, Green RM, Whitington PF. Upregulation of osteopontin expression is involved in the development of nonalcoholic steatohepatitis in a dietary murine model. Am J Physiol Gastrointest Liver Physiol. 2004 Jul;287(1):G264-73.

114. Xiao X, Gang Y, Gu Y, Zhao L, Chu J, Zhou J, Cai X, Zhang H, Xu L, Nie Y, Wu K, Liu Z, Fan D. Osteopontin contributes to TGF-beta1 mediated hepatic stellate cell activation. Dig Dis Sci. 2012;57(11):2883–91.

115. Itoh M, Suganami T, Nakagawa N, Tanaka M, Yamamoto Y, Kamei Y, Terai S, Sakaida I, Ogawa Y. Melanocortin 4 receptor-deficient mice as a novel mouse model of nonalcoholic steatohepatitis. Am J Pathol. 2011;179(5):2454–63.

116. Nakanishi Y, Tsuneyama K, Nomoto K, Fujimoto M, Salunga TL, Nakajima T, Miwa S, Murai Y, Hayashi S, Kato I, Hiraga K, Hsu DK, Liu FT, Takano Y. Nonalcoholic steatohepatitis and hepatocellular carcinoma in galectin-3 knockout mice. Hepatol Res. 2008;38(12):1241–51.

117. Watanabe S, Horie Y, Kataoka E, Sato W, Dohmen T, Ohshima S, Goto T, Suzuki A. Non-alcoholic steatohepatitis and hepatocellular carcinoma: lessons from hepatocyte-specific phosphatase and tensin homolog (PTEN)-deficient mice.

J Gastroenterol Hepatol. 2007;22 Suppl 1:S96–100.

118. Hill-Baskin AE, Markiewski MM, Buchner DA, Shao H, DeSantis D, Hsiao G, Subramaniam S, Berger NA, Croniger C, Lambris JD, Nadeau JH. Diet-induced hepatocellular carcinoma in genetically predisposed mice. Hum Mol Genet. 2009;18(16):2975–88.

119. McCullough AJ. Pathophysiology of nonalcoholic steatohepatitis. J Clin Gastroenterol. 2006 Mar;40 Suppl 1(0192–0790 (Print)):S17-29.

120. Enomoto N, Takei Y, Yamashima S, Ikejima K, Kitamura T, Sato N. Protective effect of pioglitazone against endotoxin-induced liver injury through prevention of Kupffer cell sensitization. Alcohol Clin Exp Res. 2005;29(12 Suppl):216S–9S.

121. Kawaguchi K, Sakaida I, Tsuchiya M, Omori K, Takami T, Okita K. Pioglitazone prevents hepatic steatosis, fibrosis, and enzyme-altered lesions in rat liver cirrhosis induced by a choline-deficient L-amino acid-defined diet. Biochem Biophys Res Commun. 2004;315(1):187–95.

122. Yokohama S, Yoneda M, Haneda M, Okamoto S, Okada M, Aso K, Hasegawa T, Tokusashi Y, Miyokawa N, Nakamura K. Therapeutic efficacy of an angiotensin II receptor antagonist in patients with nonalcoholic steatohepatitis. Hepatology. 2004;40(5):1222–5.

123. Torres DM, Jones FJ, Shaw JC, Williams CD, Ward JA, Harrison SA. Rosiglitazone versus rosiglitazone and metformin versus rosiglitazone and losartan in the treatment of nonalcoholic steatohepatitis in humans: a 12-month randomized, prospective, open- label trial. Hepatology. 2011;54(5):1631–9.

124. Hirose A, Ono M, Saibara T, Nozaki Y, Masuda K, Yoshioka A, Takahashi M, Akisawa N, Iwasaki S, Oben J a, Onishi S. Angiotensin II type 1 receptor blocker

inhibits fibrosis in rat nonalcoholic steatohepatitis. Hepatology. 2007 Jun;45(6):1375–81.

125. Uto H, Nakanishi C, Ido A, Hasuike S, Kusumoto K, Abe H, Numata M, Nagata K, Hayashi K, Tsubouchi H. The peroxisome proliferator-activated receptor-gamma agonist, pioglitazone, inhibits fat accumulation and fibrosis in the livers of rats fed a choline-deficient, l-amino acid-defined diet. Hepatol Res. 2005;32(4):235–42.

126. Zhang W, Wu R, Zhang F, Xu Y, Liu B, Yang Y, Zhou H, Wang L, Wan K, Xiao X, Zhang X. Thiazolidinediones improve hepatic fibrosis in rats with non-alcoholic steatohepatitis by activating the adenosine monophosphate-activated protein kinase signalling pathway. Clin Exp Pharmacol Physiol. 2012;39(12):1026–33.

127. Moreno M, Bataller R. Cytokines and renin-angiotensin system signaling in hepatic fibrosis. Clin Liver Dis. 2008;12(4):825–52, ix.

128. Yu F, Takahashi T, Moriya J, Kawaura K, Yamakawa J, Kusaka K, Itoh T, Sumino H, Morimoto S, Kanda T. Angiotensin-II receptor antagonist alleviates non-alcoholic fatty liver in KKAy obese mice with type 2 diabetes. J Int Med Res. 2006;34(3):297–302.

129. Yoshiji H, Noguchi R, Ikenaka Y, Namisaki T, Kitade M, Kaji K, Shirai Y, Yoshii J, Yanase K, Yamazaki M, Tsujimoto T, Kawaratani H, Akahane T, Aihara Y, Fukui H. Losartan, an angiotensin-II type 1 receptor blocker, attenuates the liver fibrosis development of non-alcoholic steatohepatitis in the rat. BMC Res Notes. 2009;2:70.

130. Georgescu EF. Angiotensin receptor blockers in the treatment of NASH/NAFLD:

could they be a first-class option? Adv Ther. 2008;25(11):1141–74.

131. Ashburn TT, Thor KB. Drug repositioning: Identifying and developing new uses for existing drugs. Nat Rev Drug Discov. 2004;3(8):673–83.

132. Tang W, Xu Q, Hong T, Tong G, Feng W, Shen S, Bi Y, Zhu D. Comparative efficacy of anti-diabetic agents on nonalcoholic fatty liver disease in patients with type 2 diabetes mellitus: a systematic review and meta-analysis of randomized and non-randomized studies. Diabetes Metab Res Rev. 2016 Feb;32(2):200–16.

133. Cariou B, Staels B. GFT505 for the treatment of nonalcoholic steatohepatitis and type 2 diabetes. Expert Opin Investig Drugs. 2014;23(10):1441–8.

134. Fukuda-Tsuru S, Kakimoto T, Utsumi H, Kiuchi S, Ishii S. The novel dipeptidyl peptidase-4 inhibitor teneligliptin prevents high-fat diet-induced obesity accompanied with increased energy expenditure in mice. Eur J Pharmacol. 2014;723:207–15.

135. Ideta T, Shirakami Y, Miyazaki T, Kochi T, Sakai H, Moriwaki H, Shimizu M. The Dipeptidyl Peptidase-4 Inhibitor Teneligliptin Attenuates Hepatic Lipogenesis via AMPK Activation in Non-Alcoholic Fatty Liver Disease Model Mice. Int J Mol Sci. 2015;16(12):29207–18.

136. Jung Y a., Choi YK, Jung GS, Seo HY, Kim HS, Jang BK, Kim JG, Lee IK, Kim MK, Park KG. Sitagliptin attenuates methionine/choline-deficient diet-induced steatohepatitis. Diabetes Res Clin Pract. 2014;105(1):47–57.

137. Kern M, Kloting N, Niessen HG, Thomas L, Stiller D, Mark M, Klein T, Bluher M. Linagliptin improves insulin sensitivity and hepatic steatosis in diet-induced obesity. PLoS One. 2012;7(6):e38744.

138. Klein T, Fujii M, Sandel J, Shibazaki Y, Wakamatsu K, Mark M, Yoneyama H.

Linagliptin alleviates hepatic steatosis and inflammation in a mouse model of non-alcoholic steatohepatitis. Med Mol Morphol. 2014;47(3):137–49.

139. Craddy P, Palin HJ, Johnson KI. Comparative effectiveness of dipeptidylpeptidase-4 inhibitors in type 2 diabetes: a systematic review and mixed treatment comparison. Diabetes Ther. 2014;5(1):1–41.

140. Kaku K, Katou M, Igeta M, Ohira T, Sano H. Efficacy and safety of pioglitazone added to alogliptin in Japanese patients with type 2 diabetes mellitus: a multicentre, randomized, double-blind, parallel-group, comparative study. Diabetes Obes Metab. 2015;17(12):1198–201.

141. Uchimura K, Nakamuta M, Enjoji M, Irie T, Sugimoto R, Muta T, Iwamoto H, Nawata H. Activation of retinoic X receptor and peroxisome proliferator-activated receptor-gamma inhibits nitric oxide and tumor necrosis factor-alpha production in rat Kupffer cells. Hepatology. 2001;33(1):91–9.

142. Aoki Y, Maeno T, Aoyagi K, Ueno M, Aoki F, Aoki N, Nakagawa J, Sando Y, Shimizu Y, Suga T, Arai M, Kurabayashi M. Pioglitazone, a peroxisome proliferator-activated receptor gamma ligand, suppresses bleomycin-induced acute lung injury and fibrosis. Respiration. 2009;77(3):311–9.

143. Zafiriou S, Stanners SR, Saad S, Polhill TS, Poronnik P, Pollock CA. Pioglitazone inhibits cell growth and reduces matrix production in human kidney fibroblasts. J Am Soc Nephrol. 2005;16(3):638–45.

144. Perez A, Zhao Z, Jacks R, Spanheimer R. Efficacy and safety of pioglitazone/metformin fixed-dose combination therapy compared with pioglitazone and metformin monotherapy in treating patients with T2DM. Curr Med Res Opin. 2009;25(12):2915–23.

145. Bhat A, Sebastiani G, Bhat M. Systematic review: Preventive and therapeutic applications of metformin in liver disease. World J Hepatol. 2015;7(12):1652–9.

146. Moritoh Y, Takeuchi K, Hazama M. Chronic administration of voglibose, an alpha-glucosidase inhibitor, increases active glucagon-like peptide-1 levels by increasing its secretion and decreasing dipeptidyl peptidase-4 activity in ob/ob mice. J Pharmacol Exp Ther. 2009;329(2):669–76.

147. Moritoh Y, Takeuchi K, Asakawa T, Kataoka O, Odaka H. The dipeptidyl peptidase-4 inhibitor alogliptin in combination with pioglitazone improves glycemic control, lipid profiles, and increases pancreatic insulin content in ob/ob mice. Eur J Pharmacol. 2009;602(2–3):448–54.

148. Moritoh Y, Takeuchi K, Asakawa T, Kataoka O, Odaka H. Combining a dipeptidyl peptidase-4 inhibitor, alogliptin, with pioglitazone improves glycaemic control, lipid profiles and beta-cell function in db/db mice. Br J Pharmacol. 2009;157(3):415–26.

149. Da Silva Morais A, Lebrun V, Abarca-Quinones J, Brichard S, Hue L, Guigas B, Viollet B, Leclercq I a. Prevention of steatohepatitis by pioglitazone: implication of adiponectin-dependent inhibition of SREBP-1c and inflammation. J Hepatol. 2009 Mar;50(3):489–500.

150. Lefebvre E, Moyle G, Reshef R, Richman LP, Thompson M, Hong F, Chou H, Hashiguchi T, Plato C, Poulin D, Richards T, Yoneyama H, Jenkins H, Wolfgang G, Friedman SL. Antifibrotic Effects of the Dual CCR2/CCR5 Antagonist Cenicriviroc in Animal Models of Liver and Kidney Fibrosis. PLoS One. 2016;11(6):e0158156.

151. Haukeland JW, Damås JK, Konopski Z, Løberg EM, Haaland T, Goverud I,

Torjesen P a, Birkeland K, Bjøro K, Aukrust P. Systemic inflammation in nonalcoholic fatty liver disease is characterized by elevated levels of CCL2. J Hepatol. 2006 Jun;44(6):1167–74.

152. Marra F, Tacke F. Roles for chemokines in liver disease. Gastroenterology. 2014 Jul 24;147(3):577–594 e1.

153. Miura K, Yang L, van Rooijen N, Ohnishi H, Seki E. Hepatic recruitment of macrophages promotes nonalcoholic steatohepatitis through CCR2. Am J Physiol Gastrointest Liver Physiol. 2012;302(11):G1310-21.

154. Wang X, Hausding M, Weng S-Y, Kim YO, Steven S, Klein T, Daiber A, Schuppan D. Gliptins Suppress Inflammatory Macrophage Activation to Mitigate Inflammation, Fibrosis, Oxidative Stress, and Vascular Dysfunction in Models of Nonalcoholic Steatohepatitis and Liver Fibrosis. Antioxid Redox Signal. 2018 Jan 10;28(2):87–109.

155. Itou M, Kawaguchi T, Taniguchi E, Sata M. Dipeptidyl peptidase-4: a key player in chronic liver disease. World J Gastroenterol. 2013 Apr 21;19(15):2298–306.

156. Rull A, Rodríguez F, Aragonès G, Marsillach J, Beltrán R, Alonso-Villaverde C, Camps J, Joven J. Hepatic monocyte chemoattractant protein-1 is upregulated by dietary cholesterol and contributes to liver steatosis. Cytokine. 2009;48(3):273–9.

157. Leclercq IA, Lebrun VA, Starkel P, Horsmans YJ. Intrahepatic insulin resistance in a murine model of steatohepatitis: effect of PPARgamma agonist pioglitazone. Lab Invest. 2007;87(1):56–65.

158. Moran-Salvador E, Titos E, Rius B, Gonzalez-Periz A, Garcia-Alonso V, Lopez-Vicario C, Miquel R, Barak Y, Arroyo V, Claria J. Cell-specific PPARgamma deficiency establishes anti-inflammatory and anti-fibrogenic

properties for this nuclear receptor in non-parenchymal liver cells. J Hepatol. 2013;59(5):1045–53.